Robust Data-Driven Vehicle Routing with Time Windows

Yu Zhang *

School of Business Administration, Southwestern University of Finance and Economics, China,
Department of Industrial Systems Engineering & Management, National University of Singapore, y.zhang@swufe.edu.cn

Zhenzhen Zhang *

Department of Industrial Systems Engineering & Management, National University of Singapore, isezz@nus.edu.sg

Andrew Lim

Department of Industrial Systems Engineering & Management, National University of Singapore, isealim@nus.edu.sg

Melvyn Sim

Department of Analytics & Operations, NUS Business School, dscsimm@nus.edu.sg

Optimal routing solutions based on deterministic models usually fail to deliver promised on-time services in an uncertain real world, which can lead to the loss of customers and revenue. We study a *vehicle routing problem with time windows* (VRPTW) toward the end of mitigating the risk of late customer arrivals as much as possible when travel times are based on empirical distributions. To prevent overfitting, we propose a distributionally robust optimization model that uses a Wasserstein distance–based ambiguity set to characterize ambiguous distributions that are close to the empirical distribution. Our model minimizes the decision criterion regarding delays, termed the *service fulfillment risk index* (SRI), while limiting budgeted travel costs. The SRI accounts for both the late arrival probability and its magnitude, captures the risk and ambiguity in travel times, and can be evaluated efficiently in closed form. Under the Wasserstein distance–based ambiguity, the closed-form solution reduces the VRPTW of interest to the problem under empirical travel times where all deadlines are advanced by some Wasserstein distance–related durations. To solve the problem, we develop an exact branch-and-cut approach and a variable neighborhood search meta-heuristic algorithm, and explore their speedup strategies. The effectiveness of these algorithms is established by extensive computational studies. In particular, our solution greatly improves on-time arrival performance with only modest increases in expenditures compared to the deterministic solution. Finally, our SRI also performs better during out-of-sample simulations than do the canonical decision criteria of lateness probability and expected lateness duration.

Key words: vehicle routing, Service Fulfillment Risk Index, distributionally robust optimization

History: Received November 2018; this version, April 21, 2020

---

* These authors contributed equally to this work.

1. Introduction

The Vehicle Routing Problem with Time Windows (VRPTW) involves planning and scheduling a set of vehicle routes to deliver goods or individuals to, or collect them from, customer locations—subject to vehicles' capacity constraints and customers' time window requirements. Such routing aims to reduce operational costs and/or improve service quality. The VRPTW family has broad applications in transportation and logistics; examples include express delivery, bus routing and scheduling, and waste collection.

Given the uncertain nature of travel times—especially in congested urban areas—solutions to deterministic VRPTW models usually fail, in the *execution* phase, to deliver their promised on-time service. To model uncertain travel times in the *planning* phase, traditional stochastic programming employs distribution functions, which typically cannot be obtained exactly from observations, whereas robust optimization paradigms rely on the uncertainty set of outcomes, which tend to be overly conservative. In contrast, the recently developed distributionally robust optimization can incorporate empirical distributions, permitting distributional ambiguity to avoid overfitting, and can improve out-of-sample performance compared to optimizing over empirical distributions.

Classical VRPTW models usually minimize travel costs. Although costs are reduced, compromised service quality can lead to a loss of customers and hence of revenues in the long term. With increasingly fierce competition in the contemporary market, decision makers might prefer to increase their expenditures on improving service quality and expanding market share. In order to maximize service quality, existing publications minimize the sum of late arrival probabilities at customer locations (see e.g. Adulyasak and Jaillet 2015). Yet this *lateness probability* criterion does not account for the magnitude of lateness, and its non-convexity renders computations difficult.

In articulating service loss, we introduce the *Service Fulfillment Risk Index* (SRI), which accounts not only for the late arrival probability but also for its magnitude. In addition, this index considers the distributional ambiguity of uncertain travel times, constrained by their Wasserstein distance, with reference to the empirical distribution.

Related literature

Since its introduction by Dantzig and Ramser (1959), the Vehicle Routing Problem (VRP) has received considerable interest in both academia and industry (e.g., Golden et al. 2008, Laporte 2009, Baldacci et al. 2010, Toth and Vigo 2014). One solves this problem to determine min-cost delivery routes—subject to vehicle capacity constraints—from a depot to a set of geographically dispersed customers. The VRP reduces to the Traveling Salesman Problem (TSP) when only one (uncapacitated) vehicle is considered. The VRP with Time Windows (VRPTW) involves the additional requirement that customer services must start within prescribed time windows (Cordeau

et al. 2002, Baldacci et al. 2012). A variant of VRP with flexible time windows, with penalties for servicing outside those windows, is studied by Taş et al. (2014b). If only the deadlines are imposed, then the VRPTW reduces to the VRP with Deadline (VRPD) and the TSP with Time Windows (TSPTW) reduces to the TSP with Deadline (TSPD). Extensive studies have examined the VRPTW with deterministic travel times, and various heuristic and exact algorithms have been proposed (see e.g. Lau et al. 2003, Jepsen et al. 2008, Baldacci et al. 2011, Vidal et al. 2012, Vidal et al. 2014, Pecin et al. 2017). However, situations with uncertain travel times have received relatively little attention (Oyola et al. 2016, Gendreau et al. 2016).

In *stochastic* VRPTW, the distributions of travel times are assumed to be fully known. Most previous work focuses on the TSPD (Kao 1978, Verweij et al. 2003), the VRPD (Laporte et al. 1992, Kenyon and Morton 2003), or the VRP with "soft" time windows, where services commence immediately upon arrivals and poor service ensues when arrivals occur outside the time windows (Taş et al. 2013, 2014a). For a stochastic VRPD, Laporte et al. (1992) develop a chance-constrained model to minimize operational costs while bounding the probability of late return; they demonstrate that the chance constraint can be rewritten as a deterministic constraint when travel times are normally distributed. These authors also study another model that minimizes the sum of travel and lateness penalty costs. A branch-and-cut approach is developed to solve these models. Kenyon and Morton (2003) propose models for the stochastic VRPD with two alternative objectives: minimizing the expected return time and maximizing the probability of an on-time return. They develop two branch-and-cut algorithms: the first solves the models optimally when the sample space is discrete and small; the second, for larger instances, yields suboptimal solutions via a sampling technique.

Using sample average approximation, Verweij et al. (2003) efficiently solve a stochastic TSPD by combining the Benders decomposition with branch-and-cut techniques. For a VRP with soft time windows under Gamma distributions of arc travel times, Taş et al. (2014a) develop a branch-and-price algorithm to minimize the operational cost and penalty cost incurred by time window violations. Errico et al. (2018) propose a chance-constrained model for the VRP with hard time windows and a branch-and-price-and-cut algorithm. Although these authors consider stochastic service times, their approach could be extended to handle stochastic travel times. In light of the scalability limitations of exact algorithms, several heuristics have been proposed for the stochastic VRPTW; these include, among others, saving-based constructive algorithms (Lambert et al. 1993) and tabu search (Russell and Urban 2008, Taş et al. 2013, Ehmke et al. 2015).

In *robust* VRPTW, travel times are given by an uncertainty set of outcomes. Lee et al. (2012) use the "budgeted" uncertainty set of Bertsimas and Sim (2004) to characterize travel times in a robust VRPD, where no time window should be violated in any scenario occurring within the uncertainty set, before developing a branch-and-price algorithm to solve the problem. Agra et al.

4

Zhang, Zhang, Lim, & Sim: *Robust Data-Driven Vehicle Routing*
Article Accepted by *Operations Research*; manuscript no. OPRE-2018-11-676

(2013) study a robust VRPTW and propose two models that are solved, respectively, by extending the resource and path inequalities from the deterministic to the robust optimization context and by developing a branch-and-cut algorithm and column-and-row generation.

Jaillet et al. (2016) propose using the Riskiness Index (RI) of Aumann and Serrano (2008) as a more reasonable decision criterion to evaluate the impact of late arrivals because it considers both the probability and magnitude of lateness—thereby ensuring that, the greater the tardiness, the lower the chance of it occurring. However, this approach is tractable only when arrival times can be expressed as an affine function of independently distributed factors; that requirement excludes the typical VRPTW problem, in which arrival times are piecewise linear functions of travel times. Hence Zhang et al. (2019a) replace the RI with the Essential Riskiness Index (ERI), which can be applied to the VRPTW when evaluated using empirical travel times. Yet, despite the novelties in their paper, Zhang et al. (2019a) obtain optimal solutions only for small-scale TSPTW problems (i.e., for those involving fewer than 15 nodes). The authors also propose a mean-variance distributionally robust model that results in a binary semidefinite optimization problem, which they are unable to solve within an acceptable computational time.

Contributions

We summarize our main results and contributions below.

1. **New decision criterion:** We propose a new decision criterion, termed the *Service Fulfillment Risk Index* (SRI), which provides the flexibility for the modeler to have differentiated service level in terms of probabilistic guarantee of on-time delivery.

2. **Distributional robustness with respect to empirical travel times:** We propose a distributionally robust model using Wasserstein distance–based ambiguity set to avoid overfitting to the empirical distribution and improve out-of-sample performance. We are also able to derive a closed-form solution for evaluating the SRI, which is crucial for implementations of the separation procedures in the branch-and-cut approach and of the meta-heuristic. Under this ambiguity set, we find that optimizing our VRPTW amounts to solving its counterpart under the empirical distribution when all of the deadlines are advanced by specified durations related to the Wasserstein metric distance.

3. **Improved formulation and enhancement for exact solution:** We propose a different and computationally superior formulation to that of the multi-commodity flow formulation proposed in Adulyasak and Jaillet (2015) and Zhang et al. (2019a); thus we develop a branch-and-cut algorithm to solve the model optimally. In leveraging the properties of SRI, we also introduce arc reduction and "warm start" techniques that contribute to solving larger-sized problems to optimality.

4. **Computational strategies for meta-heuristics:** We also develop a meta-heuristic algorithm to solve large-scale instances, a process that benefits from our ability to obtain closed-form solutions for evaluating the SRI. Among other advances, we use the *trie* data structure to increase computational efficiency by a factor of 15. This approach yields the same solutions as the exact algorithm for small instances, and demonstrates the ability to solve large instances.

5. **Extensive numerical study:** Because we are able to solve larger VRPTW problems than before, we can perform an extensive numerical study to evaluate the out-of-sample performance of various decision criteria in terms of mitigating the risk of service violations. We also employ k-fold cross-validation technique to calibrate the Wasserstein distance, resulting in better out-of-sample performance than that achieved by the traditional sample average approximation approach. Our proposed SRI outperforms the canonical decision criteria of lateness probability and expected lateness duration. Moreover, if travel times are uncertain then the deterministic VRPTW's "optimal" solutions tend to perform poorly against even the suboptimal SRI-based solutions that we obtain via the meta-heuristic. This result underscores the importance of the choice of decision criterion over optimality.

Overview

In Section 2 we model the VRPTW under consideration; then, in Section 3, we explain its decision criterion: our proposed Service Fulfillment Risk Index. The closed-form solution for evaluating the decision criterion is derived in Section 4. We solve the VRPTW by developing an exact branch-and-cut algorithm in Section 5 and a variable neighborhood search meta-heuristic algorithm in Section 6. Section 7 is devoted to the extensive computational studies. We conclude in Section 8 with a brief summary of our methods and findings as well as suggestions for future research. Technical proofs are relegated to EC.1 of the electronic companion.

Notation

We use $|\mathcal{A}|$ to denote the cardinality of set $\mathcal{A}$; boldface lowercase letters represent vectors. The transpose of $\boldsymbol{x}$ is denoted by $\boldsymbol{x}^\top$, and we use a tilde (˜) to represent uncertain parameters. Uncertainty is modeled via a state space Ω and a σ-algebra $\mathcal{F}$ of events on Ω. We use $\mathbb{R}$, $\mathbb{N}$, and $\mathcal{V}$ to denote the spaces of (respectively) real numbers, natural numbers, and real-valued random variables. Let $\mathcal{P}(\mathcal{W})$ represent the set of all probability distributions supported on set $\mathcal{W} \subseteq \mathbb{R}^I$. The true distribution $\mathbb{P}$ of uncertain parameters on $(\Omega, \mathcal{F})$ might not be known exactly, but instead resides in an ambiguity set $\mathcal{F}$ such that $\mathbb{P} \in \mathcal{F}$. We use $\mathbb{P}[\cdot]$ to denote the probability of some event and $\mathbb{E}_{\mathbb{P}}[\tilde{v}]$ represents the expectation of $\tilde{v}$ with probability distribution $\mathbb{P}$. Also, we put $(x)^+ = \max\{x, 0\}$.

2. Formulation of the VRPTW

The VRPTW is defined on a directed graph $\mathcal{G}' = (\mathcal{N}', \mathcal{A}')$, where $\mathcal{N}' = \{1\} \cup \mathcal{N}_c$ and $\mathcal{A}' = \{(i,j) \mid i, j \in \mathcal{N}', \ i \neq j\}$ represent the sets of nodes and arcs, respectively. Node 1 corresponds to the depot where a fleet of $m \in \mathbb{N}$ homogeneous vehicles with capacity $Q \in \mathbb{R}_+$ are based, and nodes in $\mathcal{N}_c = \{2, 3, \ldots, n\}$ represent the set of customer locations. Each node $i \in \mathcal{N}'$ is associated with a level of demand $q_i \in \mathbb{R}_+$ ($q_1 = 0$) and a time window $[\underline{\tau}_i, \overline{\tau}_i]$, where $\underline{\tau}_i \in \mathbb{R}_+$ and $\overline{\tau}_i \in \mathbb{R}_+ \cup \{+\infty\}$ prescribe (respectively) the earliest time and the latest time (i.e., the deadline) for starting the service. In particular, we let $\underline{\tau}_1 = 0$ and let $\overline{\tau}_1$ represent the deadline for returning to the depot. When a vehicle arrives at node $i \in \mathcal{N}_c$ earlier than $\underline{\tau}_i$, it waits (at no cost) and starts the service at time $\underline{\tau}_i$. However, if the arrival is later than $\overline{\tau}_i$ then the service will still be rendered but will be deemed poor. For each arc $(i,j) \in \mathcal{A}'$, the travel cost is denoted by $c_{ij} \in \mathbb{R}_+$ and the uncertain travel time by $\tilde{z}_{ij} \in \mathcal{V}_+$. We assume (without loss of generality) that, for $(i,j) \in \mathcal{A}$, the service time at node $i \in \mathcal{N}_c$ is *included* in $\tilde{z}_{ij}$.

The VRPTW requires designing at most m a priori routes to service all customers. In addition, the following four constraints must be satisfied. (i) Each vehicle, if used, departs and terminates at the depot but does not visit the depot in between; (ii) vehicle capacity is not exceeded at any location; (iii) each customer is serviced exactly once and by only one vehicle; and (iv) the total travel cost is within a budget $B \in \mathbb{R}_+$. The objective is to maximize the provision of on-time services to customers. We shall later articulate the form of this objective in more detail.

Feasible route set based on extended graph

To provide a mathematical formulation without a vehicle index, we make m "copies" of the depot for vehicles: $\mathcal{N}_d = \{n+1, n+2, \ldots, n+m\}$. We then create an extended directed graph as $\mathcal{G} = (\mathcal{N}, \mathcal{A})$, where $\mathcal{N} = \{1\} \cup \mathcal{N}_c \cup \mathcal{N}_d$ and $\mathcal{A} = \mathcal{A}_o \cup \mathcal{A}_c \cup \mathcal{A}_d$ with $\mathcal{A}_o = \{(1,j) \mid j \in \mathcal{N}_c\}$, $\mathcal{A}_c = \{(i,j) \mid i, j \in \mathcal{N}_c, i \neq j\}$, and $\mathcal{A}_d = \{(i,j) \mid i \in \mathcal{N}_c, j \in \mathcal{N}_d\}$.

In the extended graph, the attributes of nodes in $\mathcal{N}_d$—namely, $q_i = 0$, $\underline{\tau}_i = 0$, and $\overline{\tau}_i = \overline{\tau}_1$ for $i \in \mathcal{N}_d$—are copied from node 1. In case the earliest time or the deadline is not clearly prescribed for some node $i \in \mathcal{N}$, we let $\underline{\tau}_i = 0$ or $\overline{\tau}_i = +\infty$, respectively. Thus the node sets with explicit earliest time and deadline requirements are

$$\underline{\mathcal{N}} = \{i \in \mathcal{N} \mid \underline{\tau}_i > 0\} \quad \text{and} \quad \overline{\mathcal{N}} = \{i \in \mathcal{N} \mid \overline{\tau}_i < +\infty\}.$$

We analogously define the travel costs and times across arcs in $\mathcal{A}_d$ as (respectively) $c_{ij} = c_{i1}$ and $\tilde{z}_{ij} = \tilde{z}_{i1}$ for $i \in \mathcal{N}_c$ and $j \in \mathcal{N}_d$. For notational convenience, we use (i,j) and a interchangeably to

represent an arc in $\mathcal{A}$. Given any subset $\mathcal{H} \subseteq \mathcal{N}$ of nodes, the sets of their outgoing and incoming arcs can be written as

$$\delta^+(\mathcal{H}) = \{(i,j) \in \mathcal{A} \mid i \in \mathcal{H}, j \in \mathcal{N} \setminus \mathcal{H}\} \quad \text{and} \quad \delta^-(\mathcal{H}) = \{(j,i) \in \mathcal{A} \mid i \in \mathcal{H}, j \in \mathcal{N} \setminus \mathcal{H}\},$$

respectively. When $\mathcal{H}$ is a singleton, we use the notation $\delta^+(i)$ and $\delta^-(i)$ instead of $\delta^+(\{i\})$ and $\delta^-(\{i\})$. By definition of the graph, we have $\delta^+(i) = \emptyset$ for $i \in \mathcal{N}_d$ and $\delta^-(1) = \emptyset$.

We represent a feasible routing solution by the binary decision variables $\boldsymbol{x} = (x_a)_{a \in \mathcal{A}}$, where $x_a = 1$ if arc $a \in \mathcal{A}$ is traversed by some vehicle (and $x_a = 0$ otherwise). More specifically, we define the feasible region of $\boldsymbol{x}$ by

$$\mathcal{X} = \left\{ \boldsymbol{x} \in \{0,1\}^{|\mathcal{A}|} \;\middle|\; \begin{array}{ll} \displaystyle\sum_{a \in \delta^+(i)} x_a = \sum_{a \in \delta^-(i)} x_a = 1 & \forall i \in \mathcal{N}_c, \\[4mm] \displaystyle\sum_{a \in \delta^+(1)} x_a \leq m, & \\[4mm] \displaystyle\sum_{a \in \delta^-(i)} x_a \leq 1 & \forall i \in \mathcal{N}_d, \\[4mm] \displaystyle\sum_{a \in \delta^+(\mathcal{H})} x_a \geq \left\lceil \frac{\sum_{i \in \mathcal{H}} q_i}{Q} \right\rceil & \forall \mathcal{H} \subseteq \mathcal{N}_c, |\mathcal{H}| \geq 2 \end{array} \right\}. \tag{1}$$

The first constraint in (1) ensures that every customer $i \in \mathcal{N}_c$ is serviced exactly once, and the second limits the number of available vehicles. By the third constraint, at most one vehicle returns to node $i \in \mathcal{N}_d$. The last constraint is that on capacity and "subtour elimination", which is also referred to as "rounded capacity inequalities" (Lysgaard et al. 2004).

Problem formulation

Given a vehicle routing solution $\boldsymbol{x} \in \mathcal{X}$, we can extract the corresponding route(s) in the form of node sequence(s). Consider a route $(1, i_2, i_3, \ldots, i_{\kappa-1} i_\kappa, \ldots, i_{\nu-1}, i_\nu)$ that visits node $l = i_\kappa$ and ends at node $i_\nu \in \mathcal{N}_d$. As regards the partial route to l, we define the sets of visited nodes and traversed arcs as

$$\mathcal{N}_l(\boldsymbol{x}) = \{1, i_2, i_3, \ldots, i_{\kappa-1}, l\} \quad \text{and} \quad \mathcal{A}_l(\boldsymbol{x}) = \{(1, i_2), (i_2, i_3), \ldots, (i_{\kappa-1}, l)\},$$

respectively, and define the set of traversed arcs from an upstream node $k \in \mathcal{N}_l(\boldsymbol{x})$ to l as

$$\mathcal{A}_{kl}(\boldsymbol{x}) = \mathcal{A}_l(\boldsymbol{x}) \setminus \mathcal{A}_k(\boldsymbol{x}).$$

Proposition 1 *Given a routing solution $\boldsymbol{x} \in \mathcal{X}$ and a realization $\boldsymbol{z}$ of travel times $\tilde{\boldsymbol{z}}$, the service start time for each node $l \in \mathcal{N}$ is determined by the function*

$$t_l(\boldsymbol{x}, \boldsymbol{z}) = \max_{k \in \mathcal{N}_l(\boldsymbol{x})} \left\{ \underline{\tau}_k + \sum_{a \in \mathcal{A}_{kl}(\boldsymbol{x})} z_a \right\}, \tag{2}$$

Proof: See EC.1.1 of the electronic companion.

Before proceeding, we discuss a possible misconception about the expected service start time. Deterministic models seek to capture actual travel times by mean travel times, $\boldsymbol{\mu} = \mathbb{E}_{\mathbb{P}}[\tilde{\boldsymbol{z}}]$ (Toth and Vigo 2014). One could obtain the service start time $t_l(\boldsymbol{x}, \boldsymbol{\mu})$ at node $l \in \overline{\mathcal{N}}$ and then regard it as the mean value of the uncertain service start time, $\mathbb{E}_{\mathbb{P}}[t_l(\boldsymbol{x}, \tilde{\boldsymbol{z}})]$. However, Proposition 2 asserts that this equivalance does not hold in general. We illustrate the issue via an example in EC.2 of the electronic companion.

Proposition 2 *For a node $l \in \overline{\mathcal{N}}$ along one of the routes corresponding to $\boldsymbol{x}$, the service start time evaluated via mean travel times* underestimates *the mean value of the uncertain service start time. That is, $t_l(\boldsymbol{x}, \boldsymbol{\mu}) \leq \mathbb{E}_{\mathbb{P}}[t_l(\boldsymbol{x}, \tilde{\boldsymbol{z}})]$.*

Proof: Observe from Proposition 1 that $t_l(\boldsymbol{x}, \boldsymbol{z})$ is a convex piecewise affine function in $\boldsymbol{z}$. By virtue of Jensen's inequality, we have $t_l(\boldsymbol{x}, \mathbb{E}_{\mathbb{P}}[\tilde{\boldsymbol{z}}]) \leq \mathbb{E}_{\mathbb{P}}[t_l(\boldsymbol{x}, \tilde{\boldsymbol{z}})]$.   □

We next introduce the *delay function* at node $l \in \overline{\mathcal{N}}$ as

$$\xi_l(\boldsymbol{x}, \boldsymbol{z}) = t_l(\boldsymbol{x}, \boldsymbol{z}) - \overline{\tau}_l; \tag{3}$$

hence lateness occurs if and only if $\xi_l(\boldsymbol{x}, \boldsymbol{z}) > 0$. Since travel times $\tilde{\boldsymbol{z}}$ are uncertain, it follows that the delay $\xi_l(\boldsymbol{x}, \tilde{\boldsymbol{z}})$ is also uncertain.

To help decision makers design a routing plan that provides on-time services as efficiently as possible, in Section 3 we introduce the decision criterion $\rho_{\gamma_l}(\xi_l(\boldsymbol{x}, \tilde{\boldsymbol{z}})) : \mathcal{V} \mapsto [0, +\infty]$; this criterion evaluates the service fulfillment risk at node $l \in \overline{\mathcal{N}}$ in terms of the prescribed service level associated with parameter $\gamma_l \in [0, 1]$. We then propose the following model for the VRPTW:

$$\begin{aligned}
\min \ & \sum_{l \in \overline{\mathcal{N}}} \rho_{\gamma_l}(\xi_l(\boldsymbol{x}, \tilde{\boldsymbol{z}})) \\
\text{s.t. } & \boldsymbol{c}^\top \boldsymbol{x} \leq B, \\
& \boldsymbol{x} \in \mathcal{X}.
\end{aligned} \tag{4}$$

Our model minimizes the sum of the service fulfillment risk measures over all nodes with deadlines while ensuring that travel costs do not exceed the prescribed budget B. The goal is effective mitigation of the service fulfillment risk via a modest increase in budget over the minimum cost, thereby gaining market share and improving revenue in the long term. The choice of a decision criterion is obviously critical, as we explain in Section 3.

Observe that the delay function $\xi_l(\boldsymbol{x}, \boldsymbol{z})$ is convex piecewise affine in $\boldsymbol{z}$ and, in contrast to the "lifted variables" approach of Zhang et al. (2019a), here the function is not convex in the decision

variables $\boldsymbol{x}$. In Section 5 we offer a mixed-integer linear reformulation. In EC.3 of the electronic companion we propose an alternative multi-commodity flow formulation—based on Adulyasak and Jaillet (2015) and Zhang et al. (2019a)—that is compact and mixed-integer linear in form and can be solved by a Benders decomposition algorithm. Yet we show in Section 7 that our formulation (4), when solved by way of a branch-and-cut algorithm, is more computationally efficient than the multi-commodity flow formulation.

3. Service Fulfillment Risk Index

Lateness probability is perhaps the most natural decision criterion to use when measuring service fulfillment risk in routing optimization (Kenyon and Morton 2003, Adulyasak and Jaillet 2015). Despite its wide applications, this criterion may be inadequate because it does not capture the *extent* of tardiness. Furthermore, the lateness probability is a non-convex function and so is more difficult to optimize efficiently. The alternative criterion of expected lateness duration circumvents these issues, but it may not sufficiently reduce the probability of lateness (Verweij et al. 2003, Taş et al. 2014a).

To address these issues collectively, Jaillet et al. (2016) propose a decision criterion—based on the Riskiness Index of Aumann and Serrano (2008)—as follows:

$$\rho_R(\tilde{\xi}) = \min\left\{\alpha \geq 0 \,\Big|\, \sup_{\mathbb{P} \in \mathcal{F}} \mathbb{E}_{\mathbb{P}}[\exp(\tilde{\xi}/\alpha)] \leq 1\right\}.$$

The RI has several salient properties. For instance, it incorporates penalties for both the probability of tardiness and the magnitude of violation. Yet it admits a tractable formulation only if the underlying random variable $\tilde{\xi}$ can be expressed as *affine* combinations of *independently* distributed random variables, a requirement that is unsuitable in the case of empirical travel times and for modeling hard time window constraints. To resolve these issues, Zhang et al. (2019a) propose the following Essential Riskiness Index:

$$\rho_E(\tilde{\xi}) = \min\left\{\alpha \geq 0 \,\Big|\, \sup_{\mathbb{P} \in \mathcal{F}} \mathbb{E}_{\mathbb{P}}[\max\{\tilde{\xi}, -\alpha\}] \leq 0\right\}.$$

We extend this ERI by incorporating a parameter for differentiated service guarantees offered to customers, which gives modelers the flexibility to customize service levels in terms of probabilistic guarantees of on-time delivery. Our new decision criterion is defined formally as follows.

Definition 1 (Service Fulfillment Risk Index, SRI) *Given a random delay denoted by the random variable $\tilde{\xi} \in \mathcal{V}$ with probability distribution $\mathbb{P}$ and a service level $\gamma \in [0,1]$, we define the SRI, or $\rho_\gamma(\tilde{\xi}) : \mathcal{V} \mapsto [0, +\infty]$, as*

$$\rho_\gamma(\tilde{\xi}) = \min\left\{\alpha \geq 0 \,\Big|\, \mathcal{F}\text{-CVAR}_\gamma(\max\{\tilde{\xi}, -\alpha\}) \leq 0\right\}. \tag{5}$$

10

Zhang, Zhang, Lim, & Sim: *Robust Data-Driven Vehicle Routing*
Article Accepted by *Operations Research*; manuscript no. OPRE-2018-11-676

Here we follow the conventions that $\min \emptyset = +\infty$ *and* $\mathcal{F}\text{-CVAR}_\gamma(\tilde{v}) : \mathcal{V} \mapsto \mathbb{R}$ *is the worst-case Conditional Value-at-Risk (*CVAR*) over the ambiguity set* $\mathcal{F}$ *of distribution* $\mathbb{P}$:

$$\mathcal{F}\text{-CVAR}_\gamma(\tilde{v}) = \min_\beta \left\{ \beta + \frac{1}{1-\gamma} \sup_{\mathbb{P} \in \mathcal{F}} \mathbb{E}_\mathbb{P}[(\tilde{v} - \beta)^+] \right\}. \tag{6}$$

Observe that if $\gamma = 0$ then $\beta := -\infty$ is an optimal solution to the problem underlying $\mathcal{F}\text{-CVAR}_0(\tilde{v})$, in which case $\mathcal{F}\text{-CVAR}_0(\tilde{v}) = \sup_{\mathbb{P} \in \mathcal{F}} \mathbb{E}_\mathbb{P}[\tilde{v}]$. Thus the SRI is reduced to the ERI when $\gamma = 0$. This result indicates that the SRI is more "expressive" than is the ERI—although this advantage comes at the expense of introducing another decision variable β, which might well complicate the computation. Next we show that SRI does have a concise and equivalent representation that is independent of β.

Theorem 1 *The* SRI *can be equivalently represented as*

$$\rho_\gamma(\tilde{\xi}) = \min \left\{ \alpha \geq 0 \mid \sup_{\mathbb{P} \in \mathcal{F}} \mathbb{E}_\mathbb{P}[(\tilde{\xi} + \alpha)^+] \leq (1-\gamma)\alpha \right\}. \tag{7}$$

Proof: See EC.1.2 of the electronic companion.

Theorem 1 implies that SRI and ERI are similar from a computational viewpoint. The SRI also has several desirable properties, as enumerated in our next proposition.

Proposition 3 *For all* $\tilde{\xi}, \tilde{\xi}_1, \tilde{\xi}_2 \in \mathcal{V}$, *the following statements hold.*
 (i) Risk-free fulfillment: $\rho_\gamma(\tilde{\xi}) = 0$ *if and only if* $\mathbb{P}[\tilde{\xi} \leq 0] = 1$ *for all* $\mathbb{P} \in \mathcal{F}$.
 (ii) Infeasible fulfillment: *If* $\mathcal{F}\text{-CVAR}_\gamma(\tilde{\xi}) > 0$, *then* $\rho_\gamma(\tilde{\xi}) = +\infty$.
 (iii) Convexity: *For any* $\lambda \in [0,1]$, *we have* $\rho_\gamma(\lambda\tilde{\xi}_1 + (1-\lambda)\tilde{\xi}_2) \leq \lambda\rho_\gamma(\tilde{\xi}_1) + (1-\lambda)\rho_\gamma(\tilde{\xi}_2)$.
 (iv) Violation bounds:
$$\mathbb{P}[\tilde{\xi} > \rho_\gamma(\tilde{\xi})\phi] \leq \frac{1-\gamma}{1+\phi} \quad \text{for all } \phi \geq 0 \text{ and } \mathbb{P} \in \mathcal{F}.$$

Proof: See EC.1.3 of the electronic companion.

Under *risk-free fulfillment*, the SRI is equal to 0 (its best possible value) if and only if the arrival time is almost surely earlier than the deadline for all probability distributions in the ambiguity set. *Infeasible fulfillment* asserts that a route is infeasible if $\mathcal{F}\text{-CVAR}_\gamma(\tilde{\xi}) > 0$—that is, if the average service start time over the $(1-\gamma)$ tail of the worst-case distribution exceeds the deadline (Rockafellar and Uryasev 2000). *Convexity* is computationally desirable in optimization. Finally, *violation bounds* yield insights into the probability bounds of the event, namely that a service start time exceeds the deadline plus any duration. In particular, if $\phi = 0$ and $\gamma > 0$ then we can stipulate this nontrivial upper bound on the lateness probability: $\mathbb{P}[\tilde{\xi} > 0] \leq 1 - \gamma$ for all $\mathbb{P} \in \mathcal{F}$; in contrast,

Zhang, Zhang, Lim, & Sim: *Robust Data-Driven Vehicle Routing*
Article Accepted by *Operations Research*; manuscript no. OPRE-2018-11-676

11

ERI provides only the trivial bound $\mathbb{P}[\tilde{\xi} > 0] \leq 1$ (Zhang et al. 2019a). So as to offer differentiated services for customers by minimizing the sum of their SRIs in (4), the decision maker could assign a greater value of γ_l to a relatively more important customer $l \in \overline{\mathcal{N}}$.

Example 1 We illustrate the different decision criteria for several uncertain delays with two-point distributions. Table 1 reports the distributions and values of decision criteria, where M denotes some large number and we let $\gamma = 0.1$ for SRI. We observe that the lateness probability criterion is indifferent between the first two routes despite their differing magnitudes of lateness. The expected lateness duration criterion is indifferent between Routes 1 and 3, which have different lateness probabilities. Both ERI and SRI provide clear rankings of the first three routes. For Route 4, however, SRI identifies its poor performance and deems it infeasible (owing to the infeasible fulfillment property in Proposition 3) whereas ERI continues to deem it feasible. We do not report the behavior of RI because it is similar to that of ERI in this example.

Table 1   Comparison of decision criteria for several uncertain delays

Route	Uncertain delay		Decision criteria			
	Realization	Probability	Lateness probability	Expected lateness duration	ERI	SRI $(\gamma = 0.1)$
1	$-M$ 10	0.95 0.05	0.05	0.5	0.53	0.59
2	$-M$ 20	0.95 0.05	0.05	1	1.05	1.18
3	$-M$ 5	0.9 0.1	0.1	0.5	0.56	0.63
4	$-M$ 10	0.1 0.9	0.9	9	90.00	$+\infty$

Wasserstein distance–based ambiguity set

The purpose of the ambiguity set $\mathcal{F}$ in SRI is to avoid overfitting solutions to the empirical distributions. The cross-moment ambiguity set studied by Zhang et al. (2019a) leads to a computationally impractical binary semidefinite optimization formulation for their TSPTW. The alternative ϕ divergence–based ambiguity set would require that the true distribution is absolutely continuous with respect to the empirical distribution, thus ignoring any travel time scenario that has not already been observed (cf. Ben-Tal et al. 2013, Gao and Kleywegt 2016). Here we investigate a Wasserstein distance–based ambiguity set (WDAS) that circumvents these issues collectively (see e.g., Gao and Kleywegt 2016, Gao et al. 2017, Chen et al. 2018, Mohajerin Esfahani and Kuhn

2018, Zhao and Guan 2018). We show that this approach need not increase the computational complexity of our VRPTW relative to its counterpart without distributional ambiguity.

In the real world, a decision maker can never know the exact distribution $\mathbb{P}$ of travel times $\tilde{\boldsymbol{z}}$. However, the historical data $(\hat{\boldsymbol{z}}_\omega)_{\omega\in\Omega}$ may be readily accessible; here $\hat{\boldsymbol{z}}_\omega$ denotes the empirical travel times in scenario $\omega\in\Omega$, where $\Omega=\{1,2,\ldots,N\}$ is the index set. We can use the data to induce an empirical distribution $\mathbb{P}^\dagger$, or the discrete uniform distribution over the data. More precisely,

$$\mathbb{P}^\dagger[\tilde{\boldsymbol{z}}^\dagger=\hat{\boldsymbol{z}}_\omega]=\frac{1}{N}\quad\forall\omega\in\Omega,$$

where $\tilde{\boldsymbol{z}}^\dagger$ denotes the empirical travel times.

Suppose the true distribution $\mathbb{P}$ lies in a Wasserstein ball of radius $\theta\in\mathbb{R}_+$ that is centered at the empirical distribution $\mathbb{P}^\dagger$. Then the Wasserstein ambiguity set is defined as

$$\mathcal{F}(\theta)=\left\{\mathbb{P}\in\mathcal{P}(\mathcal{W})\;\middle|\;\begin{array}{l}\tilde{\boldsymbol{z}}\sim\mathbb{P},\,\tilde{\boldsymbol{z}}^\dagger\sim\mathbb{P}^\dagger,\\ d_W(\mathbb{P},\mathbb{P}^\dagger)\leq\theta\end{array}\right\}.\tag{8}$$

This paper considers the type-1 Wasserstein distance, $d_W:\mathcal{P}(\mathcal{W})\times\mathcal{P}(\mathcal{W})\mapsto[0,+\infty)$, which we define as

$$\begin{aligned}d_W(\mathbb{P},\mathbb{P}^\dagger)=\inf_{\bar{\mathbb{P}}}\;&\mathbb{E}_{\bar{\mathbb{P}}}\left[\|\tilde{\boldsymbol{z}}-\tilde{\boldsymbol{z}}^\dagger\|_p\right]\\ \text{s.t. }&(\tilde{\boldsymbol{z}},\tilde{\boldsymbol{z}}^\dagger)\sim\bar{\mathbb{P}},\\ &\tilde{\boldsymbol{z}}\sim\mathbb{P},\\ &\tilde{\boldsymbol{z}}^\dagger\sim\mathbb{P}^\dagger,\\ &\bar{\mathbb{P}}\left[(\tilde{\boldsymbol{z}},\tilde{\boldsymbol{z}}^\dagger)\in\mathcal{W}\times\mathcal{W}\right]=1.\end{aligned}\tag{9}$$

In this definition, $\bar{\mathbb{P}}$ corresponds to the joint distribution of $\tilde{\boldsymbol{z}}$ and $\tilde{\boldsymbol{z}}^\dagger$; $\mathbb{P}$ and $\mathbb{P}^\dagger$ are the marginal distributions of $\bar{\mathbb{P}}$ on (respectively) $\tilde{\boldsymbol{z}}$ and $\tilde{\boldsymbol{z}}^\dagger$; $\|\cdot\|_p$ represents a polynomial norm for which $p\geq1$; and $\mathcal{W}=\{\boldsymbol{z}\mid\boldsymbol{z}\geq\underline{\boldsymbol{z}}\}$ is the support set under consideration (here $\underline{\boldsymbol{z}}$ represents the lower bounds of $\boldsymbol{z}$).

The Wasserstein distance is a "statistical" distance between two probability distributions $\mathbb{P}$ and $\mathbb{P}^\dagger$, and it can be interpreted as the minimum total distance (with respect to the ℓ_p norm) for transporting the probability mass from $\mathbb{P}^\dagger$ to $\mathbb{P}$. Hence the ambiguity set $\mathcal{F}(\theta)$ contains all discrete and continuous probability distributions that are close to the empirical distribution. It is known that, under some mild assumptions, an appropriately chosen θ—as a function of the number N of historical data and some $\varepsilon\in(0,1)$—would guarantee (with confidence $1-\varepsilon$) that the true distribution resides in $\mathcal{F}(\theta)$. Moreover, such a choice of θ would tend to zero as N tends to infinity, indicating that the empirical distribution converges to the true distribution asympotically. We refer interested readers to Mohajerin Esfahani and Kuhn (2018) for additional details.

4. Evaluating the SRI in Closed Form

Regarding the uncertain delay at node $l \in \overline{\mathcal{N}}$ under a given routing solution $\boldsymbol{x} \in \mathcal{X}$, we are interested in evaluating its SRI, or $\rho_{\gamma_l}(\xi_l(\boldsymbol{x}, \tilde{\boldsymbol{z}}))$. According to Theorem 1, we can write

$$
\begin{aligned}
\rho_{\gamma_l}(\xi_l(\boldsymbol{x}, \tilde{\boldsymbol{z}})) = \min \ & \alpha_l \\
\text{s.t.} \ & \sup_{\mathbb{P} \in \mathcal{F}(\theta)} \mathbb{E}_{\mathbb{P}}[(\xi_l(\boldsymbol{x}, \tilde{\boldsymbol{z}}) + \alpha_l)^+] \leq (1 - \gamma_l)\alpha_l, \\
& \alpha_l \geq 0.
\end{aligned}
\tag{10}
$$

This formulation is recognized as a semi-infinite programming problem that is generally intractable (Mohajerin Esfahani and Kuhn 2018). Yet we can use duality theory to exploit this problem's structure and thus derive its tractable reformulation, as the next theorem shows.

Theorem 2 *We have* $\rho_{\gamma_l}(\xi_l(\boldsymbol{x}, \tilde{\boldsymbol{z}})) = \bar{\rho}_{\gamma_l}(\xi_l(\boldsymbol{x}, \tilde{\boldsymbol{z}})) + \frac{\theta}{1-\gamma_l}|\mathcal{A}_l(\boldsymbol{x})|^{(p-1)/p}$, *where* $\bar{\rho}_{\gamma_l}(\xi_l(\boldsymbol{x}, \tilde{\boldsymbol{z}}))$ *is the optimal value of the optimization problem*

$$
\begin{aligned}
\bar{\rho}_{\gamma_l}(\xi_l(\boldsymbol{x}, \tilde{\boldsymbol{z}})) = \min \ & \alpha_l \\
\text{s.t.} \ & \frac{1}{N} \sum_{\omega \in \Omega} \left(\xi_l(\boldsymbol{x}, \hat{\boldsymbol{z}}_\omega) + \frac{\theta}{1-\gamma_l}|\mathcal{A}_l(\boldsymbol{x})|^{(p-1)/p} + \alpha_l \right)^+ \leq (1 - \gamma_l)\alpha_l, \\
& \alpha_l \geq 0.
\end{aligned}
\tag{11}
$$

Proof: See EC.1.4 of the electronic companion. ∎

Note that problem (11) can easily be linearized and then solved as a linear optimization problem.

The closed-form evaluation

We shall derive a closed-form solution for problem (11). For notational convenience, we denote the order statistics of the empirical delays by $(\xi_l(\boldsymbol{x}, \hat{\boldsymbol{z}}_{(\omega)}))_{\omega \in \Omega}$ so that $\xi_l(\boldsymbol{x}, \hat{\boldsymbol{z}}_{(1)}) \geq \xi_l(\boldsymbol{x}, \hat{\boldsymbol{z}}_{(2)}) \geq \cdots \geq \xi_l(\boldsymbol{x}, \hat{\boldsymbol{z}}_{(N)})$. Using the result of Uryasev et al. (2010), we can calculate the CVAR of the delay under the empirical distribution as

$$
\text{CVAR}_{\gamma_l}(\xi_l(\boldsymbol{x}, \tilde{\boldsymbol{z}}^\dagger)) = \sum_{\omega=1}^{\lfloor (1-\gamma_l)N \rfloor} \frac{\xi_l(\boldsymbol{x}, \hat{\boldsymbol{z}}_{(\omega)})}{(1-\gamma_l)N} + \left(1 - \frac{\lfloor (1-\gamma_l)N \rfloor}{(1-\gamma_l)N} \right) \xi_l(\boldsymbol{x}, \hat{\boldsymbol{z}}_{(\lfloor (1-\gamma_l)N \rfloor+1)}),
\tag{12}
$$

where we put $\sum_{\omega=1}^{0} \xi_l(\boldsymbol{x}, \hat{\boldsymbol{z}}_{(\omega)}) = 0$ and $\xi_l(\boldsymbol{x}, \hat{\boldsymbol{z}}_{(N+1)}) = 0$. We are now ready to present the main result.

Theorem 3 *We have* $\rho_{\gamma_l}(\xi_l(\boldsymbol{x}, \tilde{\boldsymbol{z}})) = +\infty$ *if*

$$
\text{CVAR}_{\gamma_l}(\xi_l(\boldsymbol{x}, \tilde{\boldsymbol{z}}^\dagger)) > -\frac{\theta}{1-\gamma_l}|\mathcal{A}_l(\boldsymbol{x})|^{(p-1)/p}.
\tag{13}
$$

Otherwise,

$$
\rho_{\gamma_l}(\xi_l(\boldsymbol{x}, \tilde{\boldsymbol{z}})) = \max \left\{ \max_{i \in \{1,2,\dots,\lfloor(1-\gamma_l)N\rfloor\}} \left\{ \frac{\sum_{\omega=1}^{i} \xi_l(\boldsymbol{x}, \hat{\boldsymbol{z}}_{(\omega)}) + \theta N |\mathcal{A}_l(\boldsymbol{x})|^{(p-1)/p}}{(1-\gamma_l)N - i} \right\}, \right.
$$
$$
\left. \frac{\theta}{1-\gamma_l} |\mathcal{A}_l(\boldsymbol{x})|^{(p-1)/p} \right\}. \tag{14}
$$

Proof: See EC.1.5 of the electronic companion. ∎

Given the empirical delays $(\xi_l(\boldsymbol{x}, \hat{\boldsymbol{z}}_{(\omega)}))_{\omega \in \Omega}$ and the number $|\mathcal{A}_l(\boldsymbol{x})|$ of traversed arcs, Theorem 3 reveals that we can evaluate the SRI for node $l \in \overline{\mathcal{N}}$ by developing an efficient algorithm that first sorts the empirical delays and then checks their feasibility by calculating the CVAR. If condition (13) is satisfied, then we assert that the route is infeasible. Otherwise, we simply evaluate formula (14) to obtain the value of the SRI but without needing to solve problem (11). The computational complexity comes from sorting and is therefore of order $\mathcal{O}(N \log N)$.

Case of the ℓ_1-norm Wasserstein metric

When we use the SRI with the WDAS as the decision criterion, the VRPTW (4) can be written as

$$
\begin{aligned}
Z = \min \ & \sum_{l \in \overline{\mathcal{N}}} \alpha_l \\
\text{s.t.} \ & \sup_{\mathbb{P} \in \mathcal{F}(\theta)} \mathbb{E}_{\mathbb{P}}[(\xi_l(\boldsymbol{x}, \tilde{\boldsymbol{z}}) + \alpha_l)^+] \le (1-\gamma_l)\alpha_l \ \forall l \in \overline{\mathcal{N}}, \\
& \boldsymbol{c}^\top \boldsymbol{x} \le B, \\
& \boldsymbol{x} \in \mathcal{X}, \\
& \alpha_l \ge 0 \qquad\qquad\qquad\qquad\qquad \forall l \in \overline{\mathcal{N}}.
\end{aligned} \tag{15}
$$

So when $\theta = 0$, the Wasserstein distance–based ambiguity set shrinks to the singleton of the empirical distribution; in this case, problem (15) is reduced to a sample average approximation problem as

$$
\begin{aligned}
\min \ & \sum_{l \in \overline{\mathcal{N}}} \alpha_l \\
\text{s.t.} \ & \frac{1}{N} \sum_{\omega \in \Omega} (\xi_l(\boldsymbol{x}, \hat{\boldsymbol{z}}_\omega) + \alpha_l)^+ \le (1-\gamma_l)\alpha_l \ \forall l \in \overline{\mathcal{N}}, \\
& \boldsymbol{c}^\top \boldsymbol{x} \le B, \\
& \boldsymbol{x} \in \mathcal{X}, \\
& \alpha_l \ge 0 \qquad\qquad\qquad\qquad\qquad \forall l \in \overline{\mathcal{N}}.
\end{aligned} \tag{16}
$$

We now uncover a hidden relationship between these two problems.

Theorem 4 *Let the ℓ_1 norm be used to define the Wasserstein distance in* (9), *and suppose there is no deadline requirement for the depot (i.e., $\overline{\tau}_1 = +\infty$). Then the VRPTW* (15) *under the Wasserstein distance–based ambiguity set with some $\theta \ge 0$ gives the same solution as the VRPTW* (16) *under the empirical distribution—provided the deadline $\overline{\tau}_l$ is modified as $\overline{\tau}_l - \frac{\theta}{1-\gamma_l}$ for all $l \in \overline{\mathcal{N}}$.*

Proof: See EC.1.6 of the electronic companion. $\qquad\blacksquare$

This theorem exposes the behavior of the WDAS in an interesting situation. Using this result, a decision maker would manually modify the deadline $\overline{\tau}_l$ as $\overline{\tau}_l - \frac{\theta}{1-\gamma_l}$ in the planning phase so that, in the execution phase, the real deadline is not violated if the service start time exceeds the planned deadline for a duration of less than $\frac{\theta}{1-\gamma_l}$. We therefore interpret $\frac{\theta}{1-\gamma_l}$ as a safety time buffer that is increasing in the service level γ_l and in the radius θ of the Wasserstein ball. From the computational standpoint, Theorem 4 indicates that solving the VRPTW in this case is as easy as solving the problem under the empirical distribution—and with the advantage that pruning the solution space could then accelerate the optimization process.

5. Exact Algorithm

We first propose the following mixed-integer linear reformulation of Problem (4):

$$
\begin{aligned}
\min \ & \sum_{l\in\overline{\mathcal{N}}} \eta_l \\
\text{s.t.} \ & \sum_{a\in\mathcal{A}_l(\boldsymbol{y})} (x_a - 1)\rho_{\gamma_l}(\xi_l(\boldsymbol{y},\tilde{\boldsymbol{z}})) + \rho_{\gamma_l}(\xi_l(\boldsymbol{y},\tilde{\boldsymbol{z}})) \leq \eta_l \ \ \forall \boldsymbol{y}\in\mathcal{X}, l\in\overline{\mathcal{N}} : \rho_{\gamma_l}(\xi_l(\boldsymbol{y},\tilde{\boldsymbol{z}})) < +\infty, \\
& \sum_{a\in\mathcal{A}_l(\boldsymbol{y})} (x_a - 1) + 1 \leq 0 \qquad\qquad\qquad \forall \boldsymbol{y}\in\mathcal{X}, l\in\overline{\mathcal{N}} : \rho_{\gamma_l}(\xi_l(\boldsymbol{y},\tilde{\boldsymbol{z}})) = +\infty, \\
& \boldsymbol{c}^\top \boldsymbol{x} \leq B, \\
& \boldsymbol{x} \in \mathcal{X}, \\
& \boldsymbol{\eta} \in \mathbb{R}_+^{|\overline{\mathcal{N}}|}.
\end{aligned}
\tag{17}
$$

Here, the $\boldsymbol{\eta}$ serve as epigraphical decision variables for the SRIs. The optimality and feasibility of SRI are respectively guaranteed by the first two constraints. More specifically, for any vehicle routing solution $\boldsymbol{y}\in\mathcal{X}$, if the SRI associated with node $l\in\overline{\mathcal{N}}$ is finite then we pose the first constraint in (17). Observe that its left-hand side (LHS) is equal to the SRI, $\rho_{\gamma_l}(\xi_l(\boldsymbol{y},\tilde{\boldsymbol{z}}))$, if a route determined by $\boldsymbol{x}$ traverses the partial route (from node 1 to $l\in\overline{\mathcal{N}}$) determined by $\boldsymbol{y}$. In this case, $\eta_l = \rho_{\gamma_l}(\xi_l(\boldsymbol{x},\tilde{\boldsymbol{z}})) = \rho_{\gamma_l}(\xi_l(\boldsymbol{y},\tilde{\boldsymbol{z}}))$. Otherwise, the LHS value is nonpositive and so the constraint is redundant. Now suppose that the SRI of node $l\in\overline{\mathcal{N}}$ is infinite; then the partial route from node 1 to l and determined by $\boldsymbol{y}$ is infeasible. Hence we add the second constraint in order to rule out the routes passing through the infeasible partial route.

We can also leverage the properties of SRI to posit the following inequalities.

Proposition 4 *The constraints in* (18) *are valid for problem* (17):

$$
\mathcal{T} = \left\{ \boldsymbol{x}\in\{0,1\}^{|\mathcal{A}|} \ \middle| \
\begin{array}{ll}
\exists \boldsymbol{v}\in\mathbb{R}_+^{|\mathcal{N}|} : & \\
\underline{\tau}_i \leq v_i \leq \overline{\tau}_i & \forall i\in\mathcal{N}, \\
v_j - v_i \geq \mu_{ij} x_{ij} + (1 - x_{ij})(\underline{\tau}_j - \overline{\tau}_i) & \forall (i,j)\in\mathcal{A}
\end{array}
\right\}.
\tag{18}
$$

16

Zhang, Zhang, Lim, & Sim: *Robust Data-Driven Vehicle Routing*
Article Accepted by *Operations Research*; manuscript no. OPRE-2018-11-676

In this expression, the decision variable v_i represents the "service start time" at node $i \in \mathcal{N}$ in the deterministic world where travel times are given as empirical means: $\boldsymbol{\mu} = N^{-1} \sum_{\omega \in \Omega} \hat{\boldsymbol{z}}_\omega$.

   Proof: See EC.1.7 of the electronic companion.

   We remark that the constraints in (18) are not necessarily valid under classical decision criteria (e.g., lateness probability, expected lateness duration) because those criteria do not exhibit the infeasible fulfillment property mandated (in Proposition 3) by our SRI.

Branch-and-cut

The reformulation (17) has exponentially many constraints, so a natural way to solve it is via a branch-and-cut approach.

   We add the first two sets of constraints in (17) dynamically in a branch-and-cut fashion. Specifically, we begin by ignoring these constraints. Whenever an integer solution $\boldsymbol{x} \in \mathcal{X}$ is found, the violated constraints are separated and added; the optimal solution is obtained if no such constraint is identified. In the implementation, these constraints are added as lazy constraints through the callback function of general-purpose solvers such as the IBM ILOG CPLEX.

   Similarly, the rounded capacity inequalities (RCI) in set (1) are also added in a branch-and-cut manner. Although constraint (18) helps eliminate subtours, they cannot ensure that capacity constraints are satisfied. Furthermore, rounded capacity inequalities can accelerate this procedure since they apply also to fractional solutions. In the implementation, the RCI are separated based on the commonly used heuristic procedure of Lysgaard et al. (2004) and then added dynamically via the user-cut callback function. Yet the heuristic's nature is such that some necessary RCI might be missed. So when an integer solution is obtained, the RCI are checked *before* considering the optimality and feasibility cuts.

Arc reduction

The pre-processing technique of arc reduction, which is frequently used in deterministic VRPTW (Cordeau 2006), identifies and eliminates time window–infeasible arcs beforehand. Under uncertainty, however, it cannot be applied to VRPTW with such classical decision criteria as the probability (Kenyon and Morton 2003, Adulyasak and Jaillet 2015) and magnitude (Verweij et al. 2003, Taş et al. 2014a) of lateness. Thanks to the property of infeasible fulfillment specified in Proposition 3, the arc reduction technique is viable under our SRI decision criterion.

Proposition 5 *The following arc reduction constraints are valid:*

$$x_{jl} = 0 \quad \forall l \in \overline{\mathcal{N}}, (j,l) \in \mathcal{A} : \text{CVAR}_{\gamma_l} \left(\max\{\underline{\tau}_j + \tilde{z}_{jl}^\dagger, \underline{\tau}_l\} - \overline{\tau}_l + \frac{\theta}{1 - \gamma_l} \right) > 0;$$

$$x_{ij} + x_{jl} \le 1 \quad \forall l \in \overline{\mathcal{N}}, (i,j), (j,l) \in \mathcal{A} : \text{CVAR}_{\gamma_l} \left(\max\{\max\{\underline{\tau}_i + \tilde{z}_{ij}^\dagger, \underline{\tau}_j\} + \tilde{z}_{jl}^\dagger, \underline{\tau}_l\} - \overline{\tau}_l + \frac{\theta}{1 - \gamma_l} \right) > 0.$$

Proof: See EC.1.8 of the electronic companion.

The first and second constraints in Proposition 5 correspond to reducing one and two consecutive arcs, respectively. Although the result can be further extended to more consecutive arcs, we use only these two constraints in our computational study because they are sufficiently strong.

Warm start

We employ the meta-heuristic described in Section 6 so that we can quickly find a suboptimal—or perhaps even optimal—solution to (17) and input it as an initial solution for the branch-and-cut algorithm.

6. Meta-heuristic Algorithm

Here we describe a meta-heuristic framework that can be used to solve large-scale instances. This framework is used mainly to evaluate the performance of our proposed decision criterion.

Variable neighborhood search

The decision criterion SRI is applicable to any meta-heuristic algorithm. In this study, we use the variable neighborhood search (VNS) algorithm to demonstrate the application; we adopt the VNS because of its success in solving various VRP variants (Bräysy 2003, Kytöjoki et al. 2007, Wei et al. 2015, Lim et al. 2017). The framework is formalized as Algorithm 1.

During the entire search process, all solutions are always feasible in terms of the capacity and the SRI—although they can violate the cost budget. We therefore define and use a "penalized objective" for the solution $\boldsymbol{x}$:

$$\sum_{l \in \overline{\mathcal{N}}} \rho_\gamma(\xi_l(\boldsymbol{x}, \tilde{\boldsymbol{z}})) + M(\boldsymbol{c}^\top \boldsymbol{x} - B)^+,$$

where M is a sufficiently large number. The VNS starts from an initial solution constructed by the cheapest insertion method, which iteratively inserts the customers one by one in the best place with the least objective value. In the second loop, a neighbor solution $\boldsymbol{x}'$ is first generated by a defined neighborhood structure and is then improved by the local search procedure. If the new solution $\boldsymbol{x}''$ is better than the incumbent $\boldsymbol{x}$, then the search moves to $\boldsymbol{x}''$ and reverts to the first

---

Algorithm 1 Variable Neighborhood Search

Construct an initial solution $\boldsymbol{x}$. Initialize the best solution as $\boldsymbol{x}^* := \boldsymbol{x}$.

while the prescribed computational time limit is unreached **do**

    Initialize the index, $h := 0$.

    while $h < H$ **do**

        Set $h := h + 1$.

        Obtain a new solution $\boldsymbol{x}'$ using the hth neighborhood structure on $\boldsymbol{x}$.

        Find a solution $\boldsymbol{x}''$ by improving $\boldsymbol{x}'$ with local search.

        if $\boldsymbol{x}''$ is better than $\boldsymbol{x}$ **then**

            Set $\boldsymbol{x} := \boldsymbol{x}''$, $h := 0$.

    Update $\boldsymbol{x}^*$ if $\boldsymbol{x}$ is better.

    Generate a solution $\boldsymbol{x}$ using a diversification procedure on $\boldsymbol{x}^*$.

Output the best solution $\boldsymbol{x}^*$.

---

neighborhood structure; otherwise, it continues with the next structure. After all neighborhood structures are attempted, the starting solution is diversified (as described next) and the next loop is repeated until the stopping criterion is met.

The local search operators are *relocate*, which relocates one customer to another position; *swap*, which exchanges the positions of two customers; *2-opt*, in which a selected sequence of customers is reversed; and *2-opt**, which interchanges the end parts of two different routes. Neighborhood structures are based on the block exchange (i.e., exchanging two blocks of consecutive customers), and a series of H neighborhood structures is then designed. In the hth neighborhood structure, we perform the block exchange h times, $h = 1, 2, \ldots, H$. Diversification follows the *ruin–reconstruct* approach, which first randomly removes several customers and then rebuilds a full solution with the insertion method. This VNS is based on our previous successful implementations, which can obtain several best-known solutions for the studied VRP variants (Zhang et al. 2015, Wei et al. 2015). We refer interested readers to those papers for details.

Acceleration strategy using digital tree

To speed up the computation, we introduce the data structure "digital tree", also known as the *trie*, into our procedure. Trie is an ordered tree data structure first described by De La Briandais (1959), and it facilitates solving problems that involve time-consuming feasibility checks or calculations (Wei et al. 2015, Zhang et al. 2015) because it avoids duplicated computation of the same route—an issue that arises frequently in the search process of meta-heuristic algorithms.

The trie keeps track of the necessary information regarding each customer on the given route. Here we record the objective value SRI and the empirical service start times. For a newly obtained route $(1, i_2, i_3, \ldots, i_{\kappa-1}, i_\kappa, \ldots, i_{\nu-1}, i_\nu)$, before invoking the calculations based on Theorem 3, we first retrieve the information from the trie. Three cases are distinguished as follows.

- *Full route is retrieved:* Return the sum of objective values directly.

- *Partial route* $(1, i_2, i_3, \ldots, i_{\kappa-1})$ *is identified:* Obtain the stored objective values and the empirical service start times for customer $i_{\kappa-1}$; then calculate the service start times and objective value for every customer in $(i_\kappa, \ldots, i_{\nu-1}, i_\nu)$ and store the corresponding information in the trie.

- *The route does not exist in the trie:* Calculate the information for all customers and store it in the trie.

The trie helps avoid unnecessary calculations for duplicated full or partial routes; its use is illustrated in Figure 1. In part (a) of this figure, the current trie stores information on four routes: $(1, 2, 3, 1)$, $(1, 2, 3, 5, 1)$, $(1, 4, 1)$, and $(1, 4, 5, 1)$. If the new route to be evaluated is $(1, 2, 3, 5, 1)$, then we can retrieve the objective values from the trie directly. For the case when the new route is $(1, 2, 3, 4, 1)$, we can retrieve objective values for nodes in the partial route $(1, 2, 3)$; after that, we need only to calculate—based on the retrieved service start times at node 3—the information for customer 4 and the returning depot 1. Then the computed information is added to the trie, as shown in Figure 1(b).

(a) Store at each node the information
on SRI and empirical service start times

(b) Retrive the information
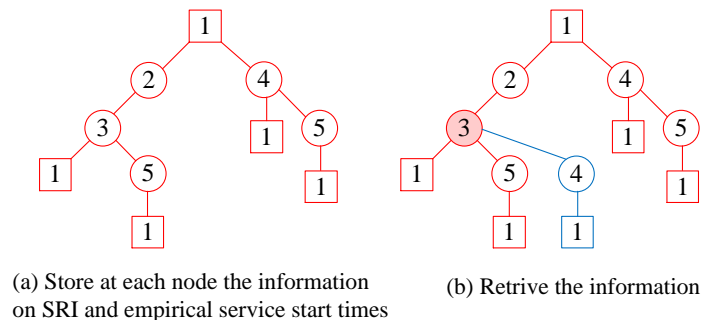
Figure 1   Structure and operation of a trie

7. Computational Studies

We report extensive computational studies to investigate the effectiveness of our decision criterion, models, and algorithms. Algorithms are coded in C++ and executed on a PC equipped with an Intel(R) Core(TM) CPU i7-7700 clocked at 3.60 GHz and 32 GB RAM running the Windows 10 operating system. The IBM ILOG CPLEX 12.6.0 is used as the mixed-integer optimization solver. The input data and source code can be found in the online supplement.

20

Zhang, Zhang, Lim, & Sim: *Robust Data-Driven Vehicle Routing*
Article Accepted by *Operations Research*; manuscript no. OPRE-2018-11-676

Instances, methods, and performance metrics

Our experiments employ Solomon's (1987) widely used instances for VRPTW. These instances involve 100 customers and are grouped into three classes according to the geographical distribution of customer locations: c (clustered), r (random), and rc (mixed). Only the instances with tight time windows are used, so there are 29 instances in total.

Since the instances are generated for the deterministic VRPTW, we modify the travel times to incorporate uncertainty. In the basic setting, for each arc $a \in \mathcal{A}$ we set the mean value μ_a of the uncertain travel time $\tilde{z}_a$ as the deterministic travel time. We assume that $\tilde{z}_a$ follows an asymmetric two-point distribution supported on $\mu_a - \sigma_a/\sqrt{3}$ and $\mu_a + \sqrt{3}\sigma_a$ with respective probabilities 0.75 and 0.25; here we generate the standard deviation $\sigma_a := \lambda_a \mu_a$ for some λ_a chosen randomly and uniformly from the interval $[0.1, 0.5]$. The two points of travel times characterize, respectively, the uncongested and congested situations. We also test several other distributions that are studied in the literature, including the uniform and triangular distributions as well as correlated distributions (Adulyasak and Jaillet 2015, Errico et al. 2018). The results and insights based on these distributions are similar to those based on the baseline two-point distributions, so we report them in EC.4 of the electronic companion.

We follow the literature in setting the number of available vehicles to 25 for all instances and in considering the number of vehicles actually used as a constraint rather than as part of the objective (Jepsen et al. 2008, Baldacci et al. 2011, Pecin et al. 2017). To compare the performance of optimal solutions derived from deterministic models, the distance between two nodes is rounded in the same way as for the existing exact algorithms—that is, rounded down to the first decimal place (Jepsen et al. 2008, Baldacci et al. 2011, Pecin et al. 2017, Zhang et al. 2019b).

The simulations allow us to compare seven different methods.

(i) *BC:* Using the branch-and-cut algorithm proposed in Section 5 to solve the mixed-integer linear optimization formulation (17). We use BC(AR), BC(WS), and BC(AR+WS) to represent the BC equipped with (respectively) the arc reduction technique, the warm start technique, and both.

(ii) *MCF:* Using the CPLEX solver to solve the multi-commodity flow formulation (EC.23) inspired by Adulyasak and Jaillet (2015) and Zhang et al. (2019a), as specified in EC.3 of the electronic companion.

(iii) *BD:* Using the Benders decomposition algorithm inspired by Zhang et al. (2019a) (and discussed in EC.3) of the electronic companion to solve (EC.23). We use BD(AR), BD(WS), and BD(AR+WS) to represent the BD combined with the three acceleration techniques named in our description of BC.

(iv) *C:* Using the exact algorithm presented by Zhang et al. (2019b) to solve the deterministic VRPTW that minimizes the total travel cost.

(v) *I:* Using the VNS meta-heuristic proposed in Section 6 to solve our problem (4).

(vi) *E:* Using the VNS to solve problem (4) with its objective function modified as the sum of expected lateness durations:

$$\sum_{l\in\overline{\mathcal{N}}}\sum_{\omega\in\Omega}\frac{(\xi_l(\boldsymbol{x},\hat{\boldsymbol{z}}_\omega))^+}{N}.$$

The studies of Verweij et al. (2003) and Taş et al. (2014a) both adopt this term as a component of the total cost to be minimized.

(vii) *P:* Using the VNS to solve problem (4) with its objective function modified as the sum of lateness probabilities:

$$\sum_{l\in\overline{\mathcal{N}}}\sum_{\omega\in\Omega}\frac{\mathbb{1}_{\{\xi_l(\boldsymbol{s},\hat{\boldsymbol{z}}_\omega)>0\}}}{N};$$

here $\mathbb{1}$ is the indicator function. Adulyasak and Jaillet (2015) adopt the same objective function to minimize.

After obtaining the vehicle routing solution, we generate another 10,000 travel time samples. We then use out-of-sample simulations to evaluate the indicators in which decision makers are usually most interested.

- *Cost:* The total travel cost, normalized to 1.

- *MaxProb:* The maximum lateness probability across all nodes.

- *SumProb:* The sum of lateness probabilities of all nodes.

- *MaxExp:* The maximum expected lateness duration across all nodes.

- *SumExp:* The sum of expected lateness durations of all nodes.

- *Early:* The sum of expected earliness durations of all nodes.

- *nLate:* The number of nodes with late services in expectation.

- *CPU:* For exact methods, the CPU time (in seconds) used by the CPLEX; for meta-heuristic methods, the CPU time that obtains the best solution for the first time.

Computational enhancement

Finding optimal solutions to large-scale instances for VRPTW under uncertain travel times is notoriously difficult. Although Adulyasak and Jaillet (2015) and Taş et al. (2014a) report some results for the case of soft time windows, the case of hard time windows—where vehicles must wait when arriving early —has not received much attention. Zhang et al. (2019a) study the problem and solve an instance with only 12 nodes. In this section we use the same instance to test the computational efficiency of the exact branch-and-cut algorithm and our acceleration strategies. See Zhang et al.

(2019a) for this instance's details, including the graph, travel times, and time windows. For the sake of consistency with the set-up of Zhang et al. (2019a), we set $\theta = 0$ and $\gamma_l = 0$, $l \in \overline{\mathcal{N}}$. We use several methods to solve this instance with varying N travel time samples; the results are presented in Table 2.

Table 2 Comparing exact methods for the instance in Zhang et al. (2019a)

Paper	Method	Number of threads	Number N of travel time samples									
			20		50		100		200		3000	
			CPU	Speed-up	CPU	Speed-up	CPU	Speed-up	CPU	Speed-up	CPU	Speed-up
Zhang et al. (2019a)	MCF	8	60	5.92	460	1.03	1684	0.29	7883	0.06	—	—
	BD	8	355	1.00	475	1.00	481	1.00	473	1.00	648	1.00
This paper	BD(AR)	8	80	4.44	143	3.32	197	2.44	258	1.83	186	3.48
	BD(WS)	8	169	2.10	333	1.43	449	1.07	454	1.04	435	1.49
	BD(AR+WS)	8	55	6.45	120	3.96	149	3.23	164	2.88	189	3.43
	BC	1	39	9.10	46	10.33	55	8.75	62	7.63	67	9.67
	BC(AR)	1	42	8.45	46	10.33	52	9.25	55	8.60	64	10.13
	BC(WS)	1	21	16.90	40	11.88	54	8.91	54	8.76	59	10.98
	BC(AR+WS)	1	30	11.83	30	15.83	59	8.15	48	9.85	53	12.23

For method MCF, the CPLEX works with eight threads. Leveraging the opportunistic parallelism provided by the CPLEX, we apply method BD—with Benders cuts added as lazy constraints—using eight threads. Since method BC adds the RCI as user cuts and since the CPLEX does not support multi-thread computing in such situations, it follows that BC runs with a single thread only. Even so, method BC generally outperforms BD in computational time, and the latter generally outperforms MCF. For method MCF, the CPU time increases super-linearly in the number N of travel time samples. However, the more sophisticated methods (BD and BC) yield only marginal improvements. Table 2 also reports the speed-up ratios relative to method BD, showing that our BC-based methods speed up by as much as an order of magnitude.

We next test the digital tree data structure's computational efficiency. Although previous tests of the trie have established its usefulness in solving some other VRP variants (e.g., the VRP with loading constraints; Zhang et al. 2015), no studies have evaluated its usage and effectiveness in solving VRPTW when travel times are uncertain. To ensure a fair comparison, we fix the number of iterations by simply improving the constructed initial solution via a local search procedure. We arbitrarily choose the instance r101 to solve while varying the number N of travel time samples. The CPU times—with and without the digital tree—are reported in Table 3.

Table 3 Comparing procedures with and without the data structure digital tree (trie)

N		8	40	200	1,000	5,000
CPU	Plain	1.04	3.07	15.37	99.14	813.74
	Trie	1.34	2.01	2.98	10.22	52.87
Speed-up		0.77	1.52	5.16	9.71	15.39

Observe that the speed-up ratio increases to 15.39 with the increment of N to 5,000, which reflects the computationally more demanding recalculation of the SRI (with complexity $\mathcal{O}(N \log N)$). The digital tree is more effective in later stages of VNS because more route information is directly available, obviating the need to recalculate the SRIs from scratch. However, the trie may be less beneficial when N is small—that is, because of the extra time spent in managing the data structure.

Comparison involving small instances

To test the meta-heuristic I's search ability, we use both exact methods and that meta-heuristic to solve the aforementioned Solomon's instances with only the first 25 customers and eight vehicles. Although the valid inequalities in Proposition 4 are computationally effective for the instance studied by Zhang et al. (2019a), they are tested ineffective vis-à-vis Solomon's instances and so we ignore those inequalities in this section. We set the CPU time limit for the exact methods at 1,800 seconds and the number N of travel time samples at 200. Results are given in Table 4, where *Obj* and *Gap* signify (respectively) the objective value and the optimality gap.

Our intention is to compare the solutions found by the meta-heuristic I with the optimal ones obtained by the exact method BC(AR). Unfortunately, the latter solves only 14 of the 29 instances optimally. For all those 14 instances, method I finds the optimal solutions. Among the remaining 15 instances, method BC(AR) obtains feasible solutions (within 1,800 seconds) for 11 instances and fails to find any solution for the other 4 instances. Among the 11 instances, our meta-heuristic I finds the same solutions as does method BC(AR) for 7 instances yet finds better solutions for the other 4 instances. These outcomes highlight the search ability of the I meta-heuristic.

We also test the exact method BC(AR+WS), which injects an initial solution to "warm start" the method BC(AR). Here we use the solution found by the meta-heuristic I with five seconds as the initial solution. Notice that method I finds the best solutions within five seconds for all the instances; the implication is that method BC(AR+WS) is only possible to obtain the same (or better) solutions than does method I. Table 4 shows that method BC(AR+WS) solves 22 out of 29 instances optimally but that it does not find better solutions (than does method I) for all the instances. For the remaining 7 instances, it is unclear whether the solutions found—within five seconds—by method I are optimal.

Comparison with classical decision criteria

Real-world VRPTWs are usually of a large scale and can seldom be solved optimally within acceptable computational times. We experiment on Solomon's instances with the first 50 and 100 customers using method BC(AR+WS); only 10 and 3 (respectively) of the 29 instances are solved optimally within 1,800 seconds. Hence we use meta-heuristics to solve the Solomon's instances and

Table 4   Comparison of heuristic versus exact methods for small instances

Instance	Method							
	I		BC(AR)			BC(AR+WS)		
	CPU	*Obj*	*CPU*	*Obj*	*Gap*	*CPU*	*Obj*	*Gap*
r101	0.07	6.38	0.11	6.38	0.00	0.14	6.38	0.00
r102	0.14	2.30	**1800.03**	2.30	**0.02**	1800.19	2.30	**0.02**
r103	0.19	0.00	**1800.00**	—	—	0.00	0.00	0.00
r104	0.07	0.00	**1800.75**	**0.90**	**1.00**	0.02	0.00	0.00
r105	0.09	1.88	5.15	1.88	0.00	2.34	1.88	0.00
r106	0.29	1.23	**1800.00**	—	—	1800.11	1.23	**1.00**
r107	4.82	0.24	**1800.32**	**1.23**	**1.00**	1800.60	0.24	**1.00**
r108	1.57	0.00	**1800.00**	—	—	0.02	0.00	0.00
r109	0.73	1.54	149.39	1.54	0.00	126.22	1.54	0.00
r110	0.56	0.00	**1800.02**	**3.56**	**1.00**	0.02	0.00	0.00
r111	3.52	0.07	**1800.05**	0.07	**1.00**	1800.13	0.07	**1.00**
r112	0.31	0.00	**1800.00**	—	—	0.02	0.00	0.00
c101	0.07	0.12	0.06	0.12	0.00	0.08	0.12	0.00
c102	0.25	0.12	3.87	0.12	0.00	1.90	0.12	0.00
c103	0.15	0.00	0.19	0.00	0.00	0.02	0.00	0.00
c104	0.25	0.00	1.58	0.00	0.00	0.02	0.00	0.00
c105	0.05	0.00	0.06	0.00	0.00	0.02	0.00	0.00
c106	0.19	3.23	0.11	3.23	0.00	0.11	3.23	0.00
c107	0.08	0.00	0.05	0.00	0.00	0.02	0.00	0.00
c108	0.07	0.00	0.25	0.00	0.00	0.02	0.00	0.00
c109	0.09	0.00	1.28	0.00	0.00	0.02	0.00	0.00
rc101	2.46	11.33	42.39	11.33	0.00	40.08	11.33	0.00
rc102	3.23	14.66	94.49	14.66	0.00	106.58	14.66	0.00
rc103	0.35	1.27	**1801.20**	**5.38**	**1.00**	1800.83	1.27	**1.00**
rc104	0.32	1.92	**1800.49**	1.92	**1.00**	1800.05	1.92	**1.00**
rc105	3.52	1.77	**1800.57**	1.77	**0.92**	1098.86	1.77	0.00
rc106	0.43	0.29	**1800.60**	0.29	**0.99**	1614.22	0.29	0.00
rc107	0.49	0.00	**1800.02**	0.00	**0.99**	889.78	0.00	0.00
rc108	0.67	0.00	**1800.03**	0.00	**1.00**	1800.11	0.00	**1.00**

compare results based on the SRI criterion with those derived using two canonical decision criteria: lateness probability and expected lateness duration.

In the experiments, we set the number N of travel time samples at 200, the budget at 1.05 times the minimum possible cost, and the CPU time limit at 900 seconds. We solve all instances with the first 25, 50, and 100 customers using methods C, I, E, and P. Table 5 reports the average results grouped by instance class. In method I we set $\theta = 0.5$ and $\gamma_l = 0.1$ for $l \in \overline{\mathcal{N}}$. We use the ℓ_1 norm to define the Wasserstein distance.

Method C minimizes the travel cost while ensuring on-time service in the deterministic world. In the presence of uncertainty, however, the out-of-sample evaluation reveals its poor on-time service performance. In particular, the lateness probability for the worst-case customer, *MaxProb*, can be greater than 50% in some instances with 100 customers. There are even customers for whom lateness occurs in expectation, a phenomenon explained by Proposition 2. Such customers might

Table 5   Comparison of decision criteria

n	Instance	Method	Performance							
			Cost	nLate	MaxProb	SumProb	MaxExp	SumExp	Early	CPU
	r1	C	1.000	0.08	0.307	0.847	2.18	4.22	221	—
		I	1.043	0.00	0.122	0.263	0.49	0.79	256	2.4
		E	1.044	0.00	0.122	0.264	0.49	0.79	261	9.7
		P	1.043	0.00	0.121	0.266	0.58	0.91	261	13.0
25	c1	C	1.000	0.00	0.063	0.112	0.28	0.42	475	—
		I	1.015	0.00	0.045	0.095	0.24	0.37	510	0.2
		E	1.019	0.00	0.045	0.095	0.24	0.37	508	0.3
		P	1.020	0.00	0.045	0.095	0.24	0.37	491	0.4
	rc1	C	1.000	0.38	0.348	1.407	3.13	10.47	91	—
		I	1.052	0.00	0.177	0.473	1.02	2.48	102	3.2
		E	1.037	0.25	0.272	0.486	1.26	2.07	90	1.1
		P	1.039	0.25	0.250	0.410	4.15	4.76	87	0.9
	r1	C	1.000	1.67	0.491	3.821	5.52	27.43	247	—
		I	1.049	0.00	0.194	0.972	1.49	4.43	312	135.1
		E	1.048	0.58	0.405	1.529	3.09	7.75	322	526.3
		P	1.047	1.00	0.697	1.423	36.02	43.53	346	161.4
50	c1	C	1.000	0.00	0.078	0.224	0.38	0.82	156	—
		I	1.016	0.00	0.054	0.161	0.26	0.58	243	2.2
		E	1.023	0.00	0.054	0.161	0.26	0.58	225	9.9
		P	1.023	0.00	0.054	0.161	0.26	0.58	216	6.6
	rc1	C	1.000	1.38	0.465	3.954	5.48	32.37	142	—
		I	1.052	0.00	0.266	1.469	2.44	8.90	182	153.4
		E	1.048	0.38	0.449	1.457	3.92	9.70	176	120.4
		P	1.048	0.88	0.510	1.185	25.70	29.66	174	151.8
	r1	C	1.000	5.25	0.582	9.119	6.05	64.05	442	—
		I	1.050	0.00	0.296	2.558	2.41	12.64	540	522.0
		E	1.049	2.83	0.843	4.900	5.82	25.89	492	378.2
		P	1.049	3.25	0.981	4.816	60.99	151.30	550	305.4
100	c1	C	1.000	1.56	0.494	1.351	4.26	9.38	60	—
		I	1.047	0.00	0.092	0.310	0.42	0.95	238	21.1
		E	1.041	0.00	0.092	0.310	0.42	0.95	174	48.7
		P	1.045	0.00	0.088	0.306	0.42	1.02	327	73.8
	rc1	C	1.000	4.88	0.515	9.619	7.14	87.86	311	—
		I	1.050	0.00	0.337	3.217	4.02	20.92	452	374.4
		E	1.049	2.88	0.757	4.847	8.19	32.42	383	529.0
		P	1.049	2.63	0.920	4.029	71.93	132.76	454	399.7

complain about the poor service and switch to another company. Similar results have been reported also by Russell and Urban (2008), Taş et al. (2013), and Ehmke et al. (2015), among others.

Under the service-oriented management philosophy, methods I, E, and P aim to improve the on-time service performance—in terms of their respective objectives—by spending 5% more and arriving earlier. Note that method I cannot obtain budget-feasible solutions for a few rc1 instances, for which greater costs are needed. It seems that c1 instances are the easiest to optimize because

their required CPU times are shorter and the on-time service performance under these methods is similar across these instances.

We next focus on r1 and rc1 instances. Table 5 documents that method I has a better overall on-time service performance than methods E and P, especially in instances with 100 customers. Since methods E and P optimize over *SumExp* and *SumProb*, respectively, we expect them to perform best in terms of their respective indicators. However, this phenomenon is observed only in the rc1 case with 25 customers. In many instances (especially those with 100 customers), method I outperforms method E with regard to *SumExp* and also outperforms method P with regard to *SumProb*. Method P achieves a lower *SumProb* than do methods C and E in most instances, but its performance is clearly suboptimal in terms of *MaxProb*, *MaxExp*, and *SumExp*. Method E is able to mitigate the lateness duration. Yet the service is biased—as shown by method E's values for *MaxProb* and *MaxExp*, which are sometimes even worse than those obtain using method C.

We believe that the favorable performance of method I benefits from the SRI properties specified in Proposition 3. In particular, the property of infeasible fulfillment greatly reduces the solution space in which customers receive poor service. So when it comes to finding a near-optimal solution, method I can be faster than methods P and E, which incorporate penalties but still allow poor services to survive in the search process. Furthermore, method I cannot sacrifice some customers to compensate for others, thus rendering robust and fair service to all customers. Hence method I's values for *MaxProb* and *MaxExp* are usually better than those derived under other methods, and *nLate* is always equal to zero in the instances tested. Owing to the convexity property of SRI, method I can be easier to search along a descent direction in local search, facilitating optimization. This advantage also explains method E performing better than method P in cases with 100 customers—that is, since the former method has a convex objective function and the latter does not. According to Proposition 3's property of violation bounds, method I accounts for both the lateness probability and its magnitude; that ability explains its balanced performance on all the on-time service indicators.

Calibrating the Wasserstein distance

The "optimizer's curse" in stochastic programming—also known, in machine learning, as overfitting—reflects that solutions based on the empirical distribution might underestimate the service fulfillment risk (Mohajerin Esfahani and Kuhn 2018). We attempt to verify this phenomenon and study the effect of incorporating distributional ambiguity to mitigate overfitting to the empirical distribution. We set the budget ratio to 1.1 instead of 1.05 in order to enlarge the feasible space, which helps elucidate the benefits of our robust data-driven optimization model.

For each θ, we solve all the r1 and rc1 instances with $N = 200$ training samples and then evaluate out-of-sample performance with another 10,000 testing samples. We fix $\gamma_l = 0.1$ ($l \in \overline{\mathcal{N}}$) and test over various Wasserstein distances θ in the discrete set $\Theta = \{0, 0.001, 0.005, 0.01, 0.05, 0.1, 0.5, 1\}$. In comparison with the set used in Mohajerin Esfahani and Kuhn's (Mohajerin Esfahani and Kuhn (2018)) computational study, our set Θ has the same range (from 0 to 1) but is sparser so as to alleviate the computational burden. We also test several $\theta > 1$; because they do not yield any additional improvements in performance, the results are not reported here. Note that the case of $\theta = 0$ ignores distributional ambiguity and corresponds to the commonly used sample average approximation. In addition, we test over a calibrated distance obtained via the k-fold cross-validation technique (for a detailed description, see Mohajerin Esfahani and Kuhn). To ease the computational burden, we apply a 4-fold cross-validation based on the average performance on instances r101, r105, r109, rc101, and rc105. In each of the four runs, we choose the best Wasserstein distance from set Θ; our calibration then amounts to averaging the four best distances. The results are presented in Table 6.

The out-of-sample SRI represents the sum of SRIs for all nodes in $\overline{\mathcal{N}}$ evaluated with the testing samples, and the in-sample counterpart is evaluated by way of our training samples. Note that the in-sample SRI coincides with the objective value of problem (4) when $\theta = 0$. We observe that, in general, the in-sample SRI optimistically underestimates the out-of-sample SRI; this is the over-fitting phenomenon. We also observe that the out-of-sample SRI tends first to decrease and then to increase—although the inherent randomness of simulation renders this tendency inconsistent. Using cross-validation as a heuristic to determine θ allows us to obtain better out-of-sample SRI than does using the empirical distribution alone. This outcome demonstrates that incorporating distributional ambiguity over empirical distributions helps improve the out-of-sample performance of predictive indicators.

8. Conclusion and Future Research

This paper details how to mitigate late service risk in Vehicle Routing Problems with Time Windows under empirical travel times. In particular, we propose a new decision criterion—the Service Fulfillment Risk Index—to measure the lateness risk. This criterion accounts for both the probability and magnitude of lateness, and its convexity makes the SRI computationally tractable. Our main theoretical result is a closed-form solution to evaluate the criterion under Wasserstein distance–based ambiguity about the empirical travel times. We also develop an exact branch-and-cut algorithm and a variable neighborhood search meta-heuristic, as well as techniques to speed them up, for solving the resultant problem. Extensive computational studies demonstrate favorable performances of our decision criterion in comparison with several existing criteria. In terms of

Table 6   Effect of the Wasserstein distance

θ	Instance	SRI (in-sample)	SRI (out-of-sample)	MaxProb	SumProb	MaxExp	SumExp	CPU
					Performance			
0	r1	6.22	6.28	0.161	1.042	1.23	4.24	591
	rc1	6.80	8.08	0.214	1.206	2.00	5.58	656
	Average	6.45	**7.00**	0.182	1.108	1.54	4.78	617
0.001	r1	6.13	6.21	0.148	0.992	1.21	4.18	652
	rc1	5.38	5.85	0.224	1.082	1.54	4.01	539
	Average	5.83	**6.07**	0.178	1.028	1.34	4.11	607
0.005	r1	6.08	6.03	0.148	0.963	1.18	4.04	612
	rc1	5.02	5.94	0.246	1.047	1.61	4.12	618
	Average	5.65	**5.99**	0.187	0.996	1.35	4.07	615
0.01	r1	6.25	6.33	0.164	1.091	1.20	4.26	524
	rc1	5.40	6.11	0.236	1.099	1.52	4.22	418
	Average	5.91	**6.24**	0.193	1.094	1.33	4.25	482
0.05	r1	6.45	6.57	0.133	1.016	1.23	4.41	600
	rc1	4.78	5.60	0.208	1.011	1.26	3.90	487
	Average	5.78	**6.18**	0.163	1.014	1.24	4.20	555
0.1	r1	6.12	6.19	0.172	1.063	1.22	4.16	413
	rc1	4.82	5.79	0.228	1.084	1.56	4.12	591
	Average	5.60	**6.03**	0.195	1.071	1.36	4.15	484
0.5	r1	6.47	6.65	0.166	1.087	1.24	4.48	494
	rc1	6.64	8.04	0.243	1.323	1.76	5.67	569
	Average	6.54	**7.21**	0.197	1.181	1.45	4.96	524
1	r1	6.62	6.83	0.160	1.006	1.26	4.58	451
	rc1	6.71	8.04	0.227	1.105	2.30	5.55	506
	Average	6.66	**7.32**	0.187	1.046	1.68	4.97	473
0.05025 (calibrated)	r1	6.07	6.14	0.147	1.024	1.20	4.15	597
	rc1	5.05	5.53	0.242	1.111	1.25	3.95	520
	Average	5.66	**5.90**	0.185	1.059	1.22	4.07	566

mitigating service violations, the deterministic model's would-be optimal solution is actually much worse than is the "suboptimal" solution obtained via our meta-heuristic with SRI. This finding points to the importance of the choice of decision criterion over optimality.

We stress that, beyond VRPTW, the set of applications in which SRI can be used to evaluate target fulfillment risk is quite broad and includes, inter alia, portfolio optimization (Natarajan et al. 2010, Li 2018), inventory control (Bertsimas and Thiele 2006, See and Sim 2010, Bandi et al. 2019), and appointment scheduling (Mak et al. 2014, Qi 2016, Jiang et al. 2017). In those problems, the uncertain attributes (financial gain, unsold inventory, patients' waiting time) can be expressed as piecewise affine functions in the uncertain parameters—respectively, the investments' returns, the demand, and service times—and so, by analogy, the closed-form result in Section 4 is applicable. It would be instructive to investigate these applications.

Zhang, Zhang, Lim, & Sim: *Robust Data-Driven Vehicle Routing*
Article Accepted by *Operations Research*; manuscript no. OPRE-2018-11-676

29

In urban areas, travel times are highly time-dependent. We do not examine this factor here but will consider it in future work.

Acknowledgments

References

Adulyasak, Y., P. Jaillet. 2015. Models and algorithms for stochastic and robust vehicle routing with deadlines. *Transportation Science* **50**(2) 608–626.

Agra, A., M. Christiansen, R. Figueiredo, L. M. Hvattum, M. Poss, C. Requejo. 2013. The robust vehicle routing problem with time windows. *Computers & Operations Research* **40**(3) 856–866.

Aumann, R. J., R. Serrano. 2008. An economic index of riskiness. *Journal of Political Economy* **116**(5) 810–836.

Baldacci, R., E. Bartolini, A. Mingozzi, R. Roberti. 2010. An exact solution framework for a broad class of vehicle routing problems. *Computational Management Science* **7**(3) 229–268.

Baldacci, R., A. Mingozzi, R. Roberti. 2011. New route relaxation and pricing strategies for the vehicle routing problem. *Operations Research* **59**(5) 1269–1283.

Baldacci, R., A. Mingozzi, R. Roberti. 2012. Recent exact algorithms for solving the vehicle routing problem under capacity and time window constraints. *European Journal of Operational Research* **218**(1) 1–6.

Bandi, C., E. Han, O. Nohadani. 2019. Sustainable inventory with robust periodic-affine policies and application to medical supply chains. *Management Science* **65**(10) 4636–4655.

Ben-Tal, A., D. Den Hertog, A. De Waegenaere, B. Melenberg, G. Rennen. 2013. Robust solutions of optimization problems affected by uncertain probabilities. *Management Science* **59**(2) 341–357.

Bertsimas, D., M. Sim. 2004. The price of robustness. *Operations Research* **52**(1) 35–53.

Bertsimas, D., A. Thiele. 2006. A robust optimization approach to inventory theory. *Operations Research* **54**(1) 150–168.

30

Zhang, Zhang, Lim, & Sim: *Robust Data-Driven Vehicle Routing*
Article Accepted by *Operations Research*; manuscript no. OPRE-2018-11-676

Boyd, S., L. Vandenberghe. 2004. *Convex Optimization*. Cambridge University Press.

Bräysy, O. 2003. A reactive variable neighborhood search for the vehicle-routing problem with time windows. *INFORMS Journal on Computing* **15**(4) 347–368.

Chen, Z., D. Kuhn, W. Wiesemann. 2018. Data-driven chance constrained programs over Wasserstein balls. *Available at Optimization Online*.

Claus, A. 1984. A new formulation for the travelling salesman problem. *SIAM Journal on Algebraic Discrete Methods* **5**(1) 21–25.

Cordeau, J.-F. 2006. A branch-and-cut algorithm for the dial-a-ride problem. *Operations Research* **54**(3) 573–586.

Cordeau, J.-F., G. Desaulniers, J. Desrosiers, M. M. Solomon, F. Soumis. 2002. VRP with time windows. *The Vehicle Routing Problem*. Society for Industrial & Applied Mathematics (SIAM), 157–193.

Dantzig, G. B., J. H. Ramser. 1959. The truck dispatching problem. *Management Science* **6**(1) 80–91.

De La Briandais, R. 1959. File searching using variable length keys. *Papers presented at the the March 3-5, 1959, Western Joint Computer Conference*. ACM, 295–298.

Ehmke, J. F., A. M. Campbell, T. L. Urban. 2015. Ensuring service levels in routing problems with time windows and stochastic travel times. *European Journal of Operational Research* **240**(2) 539–550.

Errico, F., G. Desaulniers, M. Gendreau, W. Rei, L.-M. Rousseau. 2016. A priori optimization with recourse for the vehicle routing problem with hard time windows and stochastic service times. *European Journal of Operational Research* **249**(1) 55–66.

Errico, F., G. Desaulniers, M. Gendreau, W. Rei, L.-M. Rousseau. 2018. The vehicle routing problem with hard time windows and stochastic service times. *EURO Journal on Transportation and Logistics* **7**(3) 223–251.

Gao, R., X. Chen, A. J. Kleywegt. 2017. Wasserstein distributional robustness and regularization in statistical learning. *arXiv preprint arXiv:1701.04200*.

Gao, R., A. J. Kleywegt. 2016. Distributionally robust stochastic optimization with Wasserstein distance *arXiv preprint arXiv:1701.04200*.

Gendreau, M., O. Jabali, W. Rei. 2016. 50th anniversary invited article–future research directions in stochastic vehicle routing. *Transportation Science* **50**(4) 1163–1173.

Golden, B., S. Raghavan, E. Wasil, eds. 2008. *The Vehicle Routing Problem: Latest Advances and New Challenges*. Springer US.

Jaillet, P., J. Qi, M. Sim. 2016. Routing optimization under uncertainty. *Operations Research* **64**(1) 186–200.

Jepsen, M., B. Petersen, S. Spoorendonk, D. Pisinger. 2008. Subset-row inequalities applied to the vehicle-routing problem with time windows. *Operations Research* **56**(2) 497–511.

Zhang, Zhang, Lim, & Sim: *Robust Data-Driven Vehicle Routing*
Article Accepted by *Operations Research*; manuscript no. OPRE-2018-11-676

31

Jiang, R., S. Shen, Y. Zhang. 2017. Integer programming approaches for appointment scheduling with random no-shows and service durations. *Operations Research* **65**(6) 1638–1656.

Kao, E. P. C. 1978. A preference order dynamic program for a stochastic traveling salesman problem. *Operations Research* **26**(6) 1033–1045.

Kenyon, A. S., D. P. Morton. 2003. Stochastic vehicle routing with random travel times. *Transportation Science* **37**(1) 69–82.

Kytöjoki, J., T. Nuortio, O. Bräysy, M. Gendreau. 2007. An efficient variable neighborhood search heuristic for very large scale vehicle routing problems. *Computers & Operations Research* **34**(9) 2743–2757.

Lambert, V., G. Laporte, F. Louveaux. 1993. Designing collection routes through bank branches. *Computers & Operations Research* **20**(7) 783–791.

Laporte, G. 2009. Fifty years of vehicle routing. *Transportation Science* **43**(4) 408–416.

Laporte, G., F. Louveaux, H. Mercure. 1992. The vehicle routing problem with stochastic travel times. *Transportation Science* **26**(3) 161–170.

Lau, H. C., M. Sim, K. M. Teo. 2003. Vehicle routing problem with time windows and a limited number of vehicles. *European Journal of Operational Research* **148**(3) 559–569.

Lee, C., K. Lee, S. Park. 2012. Robust vehicle routing problem with deadlines and travel time/demand uncertainty. *Journal of the Operational Research Society* **63**(9) 1294–1306.

Li, J. Y.-M. 2018. Closed-form solutions for worst-case law invariant risk measures with application to robust portfolio optimization. *Operations Research* **66**(6) 1533–1541.

Lim, A., Z. Zhang, H. Qin. 2017. Pickup and delivery service with manpower planning in Hong Kong public hospitals. *Transportation Science* **51**(2) 688–705.

Lysgaard, J., A. N. Letchford, R. W. Eglese. 2004. A new branch-and-cut algorithm for the capacitated vehicle routing problem. *Mathematical Programming* **100**(2) 423–445.

Mak, H.-Y., Y. Rong, J. Zhang. 2014. Appointment scheduling with limited distributional information. *Management Science* **61**(2) 316–334.

Mohajerin Esfahani, P., D. Kuhn. 2018. Data-driven distributionally robust optimization using the Wasserstein metric: performance guarantees and tractable reformulations. *Mathematical Programming* **171**(1) 115–166.

Natarajan, K., M. Sim, J. Uichanco. 2010. Tractable robust expected utility and risk models for portfolio optimization. *Mathematical Finance: An International Journal of Mathematics, Statistics and Financial Economics* **20**(4) 695–731.

Oyola, J., H. Arntzen, D. L. Woodruff. 2016. The stochastic vehicle routing problem, a literature review, part i: models. *EURO Journal on Transportation and Logistics* 1–29.

Pecin, D., C. Contardo, G. Desaulniers, E. Uchoa. 2017. New enhancements for the exact solution of the vehicle routing problem with time windows. *INFORMS Journal on Computing* **29**(3) 489–502.

Qi, J. 2016. Mitigating delays and unfairness in appointment systems. *Management Science* **63**(2) 566–583.

Rockafellar, R. T., S. Uryasev. 2000. Optimization of conditional value-at-risk. *Journal of Risk* **2** 21–42.

Rockafellar, R. T., S. Uryasev. 2002. Conditional value-at-risk for general loss distributions. *Journal of Banking & Finance* **26**(7) 1443–1471.

Russell, R. A., T. L. Urban. 2008. Vehicle routing with soft time windows and erlang travel times. *Journal of the Operational Research Society* **59**(9) 1220–1228.

See, C.-T., M. Sim. 2010. Robust approximation to multiperiod inventory management. *Operations Research* **58**(3) 583–594.

Solomon, M. M. 1987. Algorithms for the vehicle routing and scheduling problems with time window constraints. *Operations Research* **35**(2) 254–265.

Taş, D., M. Gendreau, N. Dellaert, T. van Woensel, A. de Kok. 2014a. Vehicle routing with soft time windows and stochastic travel times: A column generation and branch-and-price solution approach. *European Journal of Operational Research* **236**(3) 789–799.

Taş, D., N. Dellaert, T. van Woensel, T. de Kok. 2013. Vehicle routing problem with stochastic travel times including soft time windows and service costs. *Computers & Operations Research* **40**(1) 214–224.

Taş, D., O. Jabali, T. Van Woensel. 2014b. A vehicle routing problem with flexible time windows. *Computers & Operations Research* **52** 39–54.

Toth, P., D. Vigo, eds. 2014. *Vehicle Routing: Problems, Methods, and Applications, Second Edition*. Society for Industrial & Applied Mathematics (SIAM), Philadelphia.

Uryasev, S., S. Sarykalin, G. Serraino, K. Kalinchenko. 2010. VaR vs CVaR in risk management and optimization. *CARISMA Conference*.

Verweij, B., S. Ahmed, A. J. Kleywegt, G. Nemhauser, A. Shapiro. 2003. The sample average approximation method applied to stochastic routing problems: a computational study. *Computational Optimization and Applications* **24**(2-3) 289–333.

Vidal, T., T. G. Crainic, M. Gendreau, N. Lahrichi, W. Rei. 2012. A hybrid genetic algorithm for multidepot and periodic vehicle routing problems. *Operations Research* **60**(3) 611–624.

Vidal, T., T. G. Crainic, M. Gendreau, C. Prins. 2014. A unified solution framework for multi-attribute vehicle routing problems. *European Journal of Operational Research* **234**(3) 658–673.

Wei, L., Z. Zhang, D. Zhang, A. Lim. 2015. A variable neighborhood search for the capacitated vehicle routing problem with two-dimensional loading constraints. *European Journal of Operational Research* **243**(3) 798–814.

Zhang, Zhang, Lim, & Sim: *Robust Data-Driven Vehicle Routing*
Article Accepted by *Operations Research*; manuscript no. OPRE-2018-11-676

33

Zhang, Y., R. Baldacci, M. Sim, J. Tang. 2019a. Routing optimization with time windows under uncertainty. *Mathematical Programming* **175**(1-2) 263–305.

Zhang, Z., Z. Luo, H. Qin, A. Lim. 2019b. Exact algorithms for the vehicle routing problem with time windows and combinatorial auction. *Transportation Science* **53**(2) 427–441.

Zhang, Z., L. Wei, A. Lim. 2015. An evolutionary local search for the capacitated vehicle routing problem minimizing fuel consumption under three-dimensional loading constraints. *Transportation Research Part B: Methodological* **82** 20–35.

Zhao, C., Y. Guan. 2018. Data-driven risk-averse stochastic optimization with Wasserstein metric. *Operations Research Letters* **46**(2) 262–267.

Electronic Companion

EC.1. Proofs of Analytical Results

EC.1.1. Proof of Proposition 1

We can recursively calculate the service start time at node i_κ along a route $(1, i_2, i_3, \ldots, i_{\kappa-1}, i_\kappa, \ldots)$ as follows:

$$
\begin{aligned}
t_1 &= \underline{\tau}_1 = 0, \\
t_{i_2} &= \max\{t_1 + z_{1i_2}, \underline{\tau}_{i_2}\}, \\
t_{i_3} &= \max\{t_{i_2} + z_{i_2 i_3}, \underline{\tau}_{i_3}\}, \\
&\vdots \\
t_{i_\kappa} &= \max\{t_{i_{\kappa-1}} + z_{i_{\kappa-1} i_\kappa}, \underline{\tau}_{i_\kappa}\}.
\end{aligned}
$$

Accordingly, we obtain

$$
t_{i_\kappa} = \max_{i_\upsilon \in \{1, i_2, i_3, \ldots, i_{\kappa-1}, i_\kappa\}} \left\{ \underline{\tau}_{i_\upsilon} + \sum_{a \in \{(i_\upsilon, i_{\upsilon+1}), (i_{\upsilon+1}, i_{\upsilon+2}), \ldots, (i_{\kappa-1}, i_\kappa)\}} z_a \right\}. \tag{EC.1}
$$

Observe that (2) is indeed equivalent to (EC.1), in which k and l in (2) correspond to (respectively) i_υ and i_κ in (EC.1).

EC.1.2. Proof of Theorem 1

When $\gamma = 1$, it is known that $\mathcal{F}\text{-CVAR}_\gamma(\max\{\tilde{\xi}, -\alpha\}) = \max\{\operatorname{esssup}(\tilde{\xi}), -\alpha\}$. Hence, both (5) and (7) have the same solution: $\rho_\gamma(\tilde{\xi})$ is equal to zero if $\operatorname{esssup}(\tilde{\xi}) \leq 0$ or is equal to $+\infty$ otherwise.

For the other case, $\gamma \in [0, 1)$, we write SRI as an optimization problem:

$$
\begin{aligned}
\min \ &\alpha \\
\text{s.t.} \ &\beta + \frac{1}{1-\gamma} \sup_{\mathbb{P} \in \mathcal{F}} \mathbb{E}_{\mathbb{P}}[\max\{\tilde{\xi} - \beta, -\alpha - \beta, 0\}] \leq 0, \\
&\alpha \geq 0.
\end{aligned} \tag{EC.2}
$$

Denote the optimal solution by (α^*, β^*), and observe that $\beta^* \leq 0$ (because otherwise the first constraint would be violated). We now discuss two cases in greater detail.

Case 1: $\gamma = 0$. In this case, the first constraint becomes

$$
\sup_{\mathbb{P} \in \mathcal{F}} \mathbb{E}_{\mathbb{P}}[\max\{\tilde{\xi}, -\alpha, \beta\}] \leq 0.
$$

To minimize the objective α, observe that we can impose $\beta \leq -\alpha$ without changing the optimal objective value. Hence, we obtain the following equivalent form of the constraint:

$$
\sup_{\mathbb{P} \in \mathcal{F}} \mathbb{E}_{\mathbb{P}}[\max\{\tilde{\xi} + \alpha, 0\}] \leq (1-0)\alpha.
$$

This inequality gives the result.

Case 2: $\gamma \in (0,1)$. Here we prove by contradiction that $\alpha^* = -\beta^*$. Suppose first that $\alpha^* > -\beta^*$. Then, by definition, $\beta^* + \frac{1}{1-\gamma} \sup_{\mathbb{P} \in \mathcal{F}} \mathbb{E}_{\mathbb{P}}[\max\{\tilde{\xi} - \beta^*, -\alpha^* - \beta^*, 0\}] \le 0$. Now, for another solution $\hat{\alpha} := -\beta^*$ we have $\hat{\alpha} \ge 0$ because $\beta^* \le 0$. Moreover,

$$
\begin{aligned}
&\beta^* + \frac{1}{1-\gamma} \sup_{\mathbb{P} \in \mathcal{F}} \mathbb{E}_{\mathbb{P}}[\max\{\tilde{\xi} - \beta^*, -\hat{\alpha} - \beta^*, 0\}] \\
&= \beta^* + \frac{1}{1-\gamma} \sup_{\mathbb{P} \in \mathcal{F}} \mathbb{E}_{\mathbb{P}}[\max\{\tilde{\xi} - \beta^*, 0\}] && (\text{because } -\hat{\alpha} - \beta^* = 0) \\
&= \beta^* + \frac{1}{1-\gamma} \sup_{\mathbb{P} \in \mathcal{F}} \mathbb{E}_{\mathbb{P}}[\max\{\tilde{\xi} - \beta^*, -\alpha^* - \beta^*, 0\}] && (\text{because } \alpha^* > -\beta^*) \\
&\le 0.
\end{aligned}
$$

Hence $\hat{\alpha}$ is feasible and achieves a lower objective value, which contradicts the statement that α^* is optimal.

Suppose instead that $\alpha^* < -\beta^*$. We claim that $\hat{\beta} := -\alpha^*$ is a feasible solution because

$$
\begin{aligned}
&\hat{\beta} + \frac{1}{1-\gamma} \sup_{\mathbb{P} \in \mathcal{F}} \mathbb{E}_{\mathbb{P}}[\max\{\tilde{\xi} - \hat{\beta}, -\alpha^* - \hat{\beta}, 0\}] \\
&= \hat{\beta} + \frac{1}{1-\gamma} \sup_{\mathbb{P} \in \mathcal{F}} \mathbb{E}_{\mathbb{P}}[\max\{\tilde{\xi} - \hat{\beta}, -\alpha^* - \hat{\beta}\}] \\
&= \beta^* + (\hat{\beta} - \beta^*) + \frac{1}{1-\gamma} \sup_{\mathbb{P} \in \mathcal{F}} \mathbb{E}_{\mathbb{P}}[\max\{\tilde{\xi} - \beta^* - (\hat{\beta} - \beta^*), -\alpha^* - \beta^* - (\hat{\beta} - \beta^*)\}] \\
&= \beta^* + \frac{1}{1-\gamma} \sup_{\mathbb{P} \in \mathcal{F}} \mathbb{E}_{\mathbb{P}}[\max\{\tilde{\xi} - \beta^*, -\alpha^* - \beta^*\}] + \left(1 - \frac{1}{1-\gamma}\right)(\hat{\beta} - \beta^*) \\
&= \beta^* + \frac{1}{1-\gamma} \sup_{\mathbb{P} \in \mathcal{F}} \mathbb{E}_{\mathbb{P}}[\max\{\tilde{\xi} - \beta^*, -\alpha^* - \beta^*, 0\}] + \left(1 - \frac{1}{1-\gamma}\right)(\hat{\beta} - \beta^*) \\
&\le \left(1 - \frac{1}{1-\gamma}\right)(\hat{\beta} - \beta^*) \\
&< 0.
\end{aligned}
$$

Since the constraint is not tight when $\beta := \hat{\beta}$, there must exist some $\hat{\alpha} < \alpha^*$ that will make the constraint tight; hence $\hat{\alpha}$ attains a lower objective value than does α^*, which contradicts the statement that α^* is optimal. To conclude: $\beta^* = -\alpha^*$, and the first constraint of (EC.2) is equivalent to

$$
-\alpha + \frac{1}{1-\gamma} \sup_{\mathbb{P} \in \mathcal{F}} \mathbb{E}_{\mathbb{P}}[\max\{\tilde{\xi} + \alpha, 0\}] \le 0,
$$

which is exactly the constraint in (7). The result now follows.

EC.1.3. Proof of Proposition 3

We seek to establish the following properties for all $\tilde{\xi}, \tilde{\xi}_1, \tilde{\xi}_2 \in \mathcal{V}$.

(i) *Risk-free fulfillment.* If $\mathbb{P}[\tilde{\xi} \le 0] = 1$ for all $\mathbb{P} \in \mathcal{F}$, then the constraint $\sup_{\mathbb{P} \in \mathcal{F}} \mathbb{E}_{\mathbb{P}}[(\tilde{\xi} + \alpha)^+] \le (1-\gamma)\alpha$ applies for $\alpha = 0$. Therefore, $\rho_\gamma(\tilde{\xi}) = 0$. If, conversely, $\rho_\gamma(\tilde{\xi}) = 0$ then $\sup_{\mathbb{P} \in \mathcal{F}} \mathbb{E}_{\mathbb{P}}[(\tilde{\xi})^+] \le 0$ and so $\mathbb{P}[\tilde{\xi} \le 0] = 1$ for all $\mathbb{P} \in \mathcal{F}$.

(ii) *Infeasible fulfillment.* For any $\alpha \in [0, +\infty)$, if $\mathcal{F}\text{-CVAR}_\gamma(\tilde{\xi}) > 0$ then $\mathcal{F}\text{-CVAR}_\gamma(\max\{\tilde{\xi}, -\alpha\}) > 0$. However, the definition of SRI requires that $\mathcal{F}\text{-CVAR}_\gamma(\max\{\tilde{\xi}, -\alpha\}) \le 0$; therefore, $\rho_\gamma(\tilde{\xi}) = \min \emptyset = +\infty$.

(iii) *Convexity.* Put $\alpha_1^* = \rho_\gamma(\tilde{\xi}_1)$ and $\alpha_2^* = \rho_\gamma(\tilde{\xi}_2)$. By definition, we have $\sup_{\mathbb{P}\in\mathcal{F}} \mathbb{E}_\mathbb{P}[(\tilde{\xi}_1 + \alpha_1^*)^+] - (1 - \gamma)\alpha_1^* \leq 0$ and $\sup_{\mathbb{P}\in\mathcal{F}} \mathbb{E}_\mathbb{P}[(\tilde{\xi}_2 + \alpha_2^*)^+] - (1 - \gamma)\alpha_2^* \leq 0$. Observe that the function $\sup_{\mathbb{P}\in\mathcal{F}} \mathbb{E}_\mathbb{P}[(\tilde{\xi} + \alpha)^+] - (1 - \gamma)\alpha$ is jointly convex in $\tilde{\xi}$ and α—from which it follows that, for $\lambda \in [0, 1]$,

$$
\begin{aligned}
\sup_{\mathbb{P}\in\mathcal{F}} &\, \mathbb{E}_\mathbb{P}\big[\big((\lambda\tilde{\xi}_1 + (1-\lambda)\tilde{\xi}_2) + (\lambda\alpha_1^* + (1-\lambda)\alpha_2^*)\big)^+\big] - (1-\gamma)\left(\lambda\alpha_1^* + (1-\lambda)\alpha_2^*\right) \\
&\leq \lambda\left(\sup_{\mathbb{P}\in\mathcal{F}} \mathbb{E}_\mathbb{P}[(\tilde{\xi}_1 + \alpha_1^*)^+] - (1-\gamma)\alpha_1^*\right) + (1-\lambda)\left(\sup_{\mathbb{P}\in\mathcal{F}} \mathbb{E}_\mathbb{P}[(\tilde{\xi}_2 + \alpha_2^*)^+] - (1-\gamma)\alpha_2^*\right) \\
&\leq 0.
\end{aligned}
$$

As a result, $\alpha_\lambda = \lambda\alpha_1^* + (1-\lambda)\alpha_2^*$ satisfies the constraint $\sup_{\mathbb{P}\in\mathcal{F}} \mathbb{E}_\mathbb{P}[(\lambda\tilde{\xi}_1 + (1-\lambda)\tilde{\xi}_2 + \alpha_\lambda)^+] \leq (1-\gamma)\alpha_\lambda$ and so $\rho_\gamma(\lambda\tilde{\xi}_1 + (1-\lambda)\tilde{\xi}_2) \leq \alpha_\lambda = \lambda\rho_\gamma(\tilde{\xi}_1) + (1-\lambda)\rho_\gamma(\tilde{\xi}_2)$.

(iv) *Violation bounds.* The bound applies for $\rho_\gamma(\tilde{\xi}) = \infty$ and $\rho_\gamma(\tilde{\xi}) = 0$ because the latter would indicate that $\mathbb{P}[\tilde{\xi} > 0] = 0$ for all $\mathbb{P} \in \mathcal{F}$. For the case $\rho_\gamma(\tilde{\xi}) \in (0, +\infty)$, let $\alpha^* = \rho_\gamma(\tilde{\xi})$; then, for $\mathbb{P} \in \mathcal{F}$, we have

$$
\begin{aligned}
\mathbb{P}[\tilde{\xi} > \alpha^*\phi] = \mathbb{P}[\tilde{\xi} + \alpha^* > \alpha^*\phi + \alpha^*] \\
\leq \mathbb{P}[(\tilde{\xi} + \alpha^*)^+ > \alpha^*(1 + \phi)] \\
\leq \frac{\mathbb{E}[(\tilde{\xi} + \alpha^*)^+]}{\alpha^*(1 + \phi)} \\
\leq \frac{(1 - \gamma)\alpha^*}{\alpha^*(1 + \phi)} \\
= \frac{1 - \gamma}{1 + \phi}.
\end{aligned}
$$

The second and third inequalities hold by Markov's inequality and the representation (7), respectively.

EC.1.4. Proof of Theorem 2

To streamline the notation, in this proof we omit the l subscript provided no confusion could arise. The proof proceeds in three steps. The first step follows standard arguments from the literature; the second and third steps rely on our observations of the special model structure.

Step 1: Derive a tractable reformulation of the term $\sup_{\mathbb{P}\in\mathcal{F}(\theta)} \mathbb{E}_\mathbb{P}[(\xi(\boldsymbol{x}, \tilde{\boldsymbol{z}}) + \alpha)^+]$. This term can be written more explicitly as

$$
\begin{aligned}
Z_1 = \sup \;\; &\mathbb{E}_\mathbb{P}[(\xi(\boldsymbol{x}, \tilde{\boldsymbol{z}}) + \alpha)^+] \\
\text{s.t.} \;\; &\mathbb{E}_{\bar{\mathbb{P}}}[\|\tilde{\boldsymbol{z}} - \tilde{\boldsymbol{z}}^\dagger\|_p] \leq \theta, \\
&(\tilde{\boldsymbol{z}}, \tilde{\boldsymbol{z}}^\dagger) \sim \bar{\mathbb{P}}, \\
&\tilde{\boldsymbol{z}} \sim \mathbb{P}, \\
&\tilde{\boldsymbol{z}}^\dagger \sim \mathbb{P}^\dagger, \\
&\bar{\mathbb{P}}[(\tilde{\boldsymbol{z}}, \tilde{\boldsymbol{z}}^\dagger) \in \mathcal{W} \times \mathcal{W}] = 1.
\end{aligned} \tag{EC.3}
$$

In light of the law of total probability, we can construct the joint distribution $\bar{\bar{\mathbb{P}}}$ of $\tilde{z}^{\dagger}$ and $\tilde{z}$ using the marginal distribution $\mathbb{P}^{\dagger}$ of $\tilde{z}^{\dagger}$ and the conditional distribution $\mathbb{P}_{\omega}$ of $\tilde{z}$ when $\tilde{z}^{\dagger} = \hat{z}_{\omega}$ for all $\omega \in \Omega$. Therefore, problem (EC.3) can be equivalently expressed as

$$Z_1 = \sup \frac{1}{N} \sum_{\omega \in \Omega} \mathbb{E}_{\mathbb{P}_{\omega}}[(\xi(\boldsymbol{x}, \tilde{z}) + \alpha)^+]$$
$$\text{s.t. } \frac{1}{N} \sum_{\omega \in \Omega} \mathbb{E}_{\mathbb{P}_{\omega}}[\|\tilde{z} - \hat{z}_{\omega}\|_p] \leq \theta,$$
$$\mathbb{P}_{\omega}[\tilde{z} \in \mathcal{W}] = 1 \qquad \forall \omega \in \Omega$$

or, more explicitly, as

$$Z_1 = \sup \frac{1}{N} \sum_{\omega \in \Omega} \int_{\mathcal{W}} \left((\xi(\boldsymbol{x}, \boldsymbol{z}) + \alpha)^+ \right) \mathrm{d}F_{\omega}(\boldsymbol{z})$$
$$\text{s.t. } \frac{1}{N} \sum_{\omega \in \Omega} \int_{\mathcal{W}} (\|\boldsymbol{z} - \hat{z}_{\omega}\|_p) \mathrm{d}F_{\omega}(\boldsymbol{z}) \leq \theta, \tag{EC.4}$$
$$\frac{1}{N} \int_{\mathcal{W}} \mathrm{d}F_{\omega}(\boldsymbol{z}) = \frac{1}{N} \qquad \forall \omega \in \Omega,$$
$$\mathrm{d}F_{\omega}(\boldsymbol{z}) \geq 0 \qquad \forall \omega \in \Omega,\, \boldsymbol{z} \in \mathcal{W};$$

here $F_{\omega}(\boldsymbol{z})$ denotes the cumulative distribution function of the travel times. This problem has infinitely many decision variables $\mathrm{d}F_{\omega}(\boldsymbol{z})$, so we address (EC.4) by investigating its dual problem as

$$D_1 = \inf \theta r + \frac{1}{N} \sum_{\omega \in \Omega} v_{\omega}$$
$$\text{s.t. } v_{\omega} + r\|\boldsymbol{z} - \hat{z}_{\omega}\|_p \geq (\xi(\boldsymbol{x}, \boldsymbol{z}) + \alpha)^+ \; \forall \omega \in \Omega,\, \boldsymbol{z} \in \mathcal{W}, \tag{EC.5}$$
$$r \in \mathbb{R}_+,$$
$$v_{\omega} \in \mathbb{R} \qquad \forall \omega \in \Omega.$$

Since the support set $\mathcal{W}$ is a polyhedron and since the "loss function" $(\xi(\boldsymbol{x}, \boldsymbol{z}) + \alpha)^+$ is convex piecewise affine in $\boldsymbol{z}$, it follows from Mohajerin Esfahani and Kuhn (2018, Cor. 5.1) that strong duality holds for (EC.4). Therefore, $Z_1 = D_1$.

The technical difficulty in solving problem (EC.5) lies in addressing the first constraint. Given any vehicle routing solution $\boldsymbol{x} \in \mathcal{X}$, let $\nu_{kla}(\boldsymbol{x}) = 1$ if $a \in \mathcal{A}_{kl}(\boldsymbol{x})$ and $\nu_{kla}(\boldsymbol{x}) = 0$ otherwise; then $\sum_{a \in \mathcal{A}_{kl}(\boldsymbol{x})} z_a = \boldsymbol{\nu}_{kl}(\boldsymbol{x})^\top \boldsymbol{z}$. Hence the first constraint is equivalent to

$$\begin{cases} v_{\omega} + r\|\boldsymbol{z} - \hat{z}_{\omega}\|_p \geq \underline{\tau}_k + \boldsymbol{\nu}_{kl}(\boldsymbol{x})^\top \boldsymbol{z} - \overline{\tau}_l + \alpha \; \forall \omega \in \Omega,\, k \in \mathcal{N}_l(\boldsymbol{x}),\, \boldsymbol{z} \in \mathcal{W}, \\ v_{\omega} + r\|\boldsymbol{z} - \hat{z}_{\omega}\|_p \geq 0 \qquad\qquad\qquad\qquad\qquad \forall \omega \in \Omega,\, \boldsymbol{z} \in \mathcal{W} \end{cases}$$

$$\iff \begin{cases} v_{\omega} + \max_{\|\boldsymbol{y}_{\omega k}\|_{\frac{p}{p-1}} \leq r} \boldsymbol{y}_{\omega k}^\top(\boldsymbol{z} - \hat{z}_{\omega}) \geq \underline{\tau}_k + \boldsymbol{\nu}_{kl}(\boldsymbol{x})^\top \boldsymbol{z} - \overline{\tau}_l + \alpha \; \forall \omega \in \Omega,\, k \in \mathcal{N}_l(\boldsymbol{x}),\, \boldsymbol{z} \in \mathcal{W}, \\ v_{\omega} + \max_{\|\boldsymbol{y}_{\omega 0}\|_{\frac{p}{p-1}} \leq r} \boldsymbol{y}_{\omega 0}^\top(\boldsymbol{z} - \hat{z}_{\omega}) \geq 0 \qquad\qquad\qquad \forall \omega \in \Omega,\, \boldsymbol{z} \in \mathcal{W} \end{cases}$$

$$\iff \begin{cases} (\boldsymbol{y}_{\omega k} - \boldsymbol{\nu}_{kl}(\boldsymbol{x}))^\top \boldsymbol{z} \geq \boldsymbol{y}_{\omega k}^\top \hat{z}_{\omega} + \underline{\tau}_k - \overline{\tau}_l + \alpha - v_{\omega} \; \forall \omega \in \Omega,\, k \in \mathcal{N}_l(\boldsymbol{x}),\, \boldsymbol{z} \in \mathcal{W}, \\ \boldsymbol{y}_{\omega 0}^\top \boldsymbol{z} \geq \boldsymbol{y}_{\omega 0}^\top \hat{z}_{\omega} - v_{\omega} \qquad\qquad\qquad\qquad\qquad \forall \omega \in \Omega,\, \boldsymbol{z} \in \mathcal{W}, \\ \|\boldsymbol{y}_{\omega k}\|_{\frac{p}{p-1}} \leq r \qquad\qquad\qquad\qquad\qquad\qquad\quad \forall \omega \in \Omega,\, k \in \mathcal{N}_l(\boldsymbol{x}) \cup \{0\} \end{cases}$$

$$\Longleftrightarrow \begin{cases} \min_{\boldsymbol{z} \geq \underline{\boldsymbol{z}}} (\boldsymbol{y}_{\omega k} - \boldsymbol{\nu}_{kl}(\boldsymbol{x}))^{\top} \boldsymbol{z} \geq \boldsymbol{y}_{\omega k}^{\top} \hat{\boldsymbol{z}}_{\omega} + \underline{\tau}_k - \overline{\tau}_l + \alpha - v_{\omega} & \forall \omega \in \Omega, \ k \in \mathcal{N}_l(\boldsymbol{x}), \\ \min_{\boldsymbol{z} \geq \underline{\boldsymbol{z}}} \boldsymbol{y}_{\omega 0}^{\top} \boldsymbol{z} \geq \boldsymbol{y}_{\omega 0}^{\top} \hat{\boldsymbol{z}}_{\omega} - v_{\omega} & \forall \omega \in \Omega, \\ \|\boldsymbol{y}_{\omega k}\|_{\frac{p}{p-1}} \leq r & \forall \omega \in \Omega, \ k \in \mathcal{N}_l(\boldsymbol{x}) \cup \{0\} \end{cases}$$

$$\Longleftrightarrow \begin{cases} \max\limits_{\substack{\boldsymbol{q}_{\omega k} = \boldsymbol{y}_{\omega k} - \boldsymbol{\nu}_{kl}(\boldsymbol{x}) \\ \boldsymbol{q}_{\omega k} \geq \boldsymbol{0}}} \underline{\boldsymbol{z}}^{\top} \boldsymbol{q}_{\omega k} \geq \boldsymbol{y}_{\omega k}^{\top} \hat{\boldsymbol{z}}_{\omega} + \underline{\tau}_k - \overline{\tau}_l + \alpha - v_{\omega} & \forall \omega \in \Omega, \ k \in \mathcal{N}_l(\boldsymbol{x}), \\ \max\limits_{\substack{\boldsymbol{q}_{\omega 0} = \boldsymbol{y}_{\omega 0} \\ \boldsymbol{q}_{\omega 0} \geq \boldsymbol{0}}} \underline{\boldsymbol{z}}^{\top} \boldsymbol{q}_{\omega 0} \geq \boldsymbol{y}_{\omega 0}^{\top} \hat{\boldsymbol{z}}_{\omega} - v_{\omega} & \forall \omega \in \Omega, \\ \|\boldsymbol{y}_{\omega k}\|_{\frac{p}{p-1}} \leq r & \forall \omega \in \Omega, \ k \in \mathcal{N}_l(\boldsymbol{x}) \cup \{0\} \end{cases}$$

$$\Longleftrightarrow \begin{cases} \underline{\boldsymbol{z}}^{\top} \boldsymbol{q}_{\omega k} \geq \boldsymbol{y}_{\omega k}^{\top} \hat{\boldsymbol{z}}_{\omega} + \underline{\tau}_k - \overline{\tau}_l + \alpha - v_{\omega} & \forall \omega \in \Omega, \ k \in \mathcal{N}_l(\boldsymbol{x}), \\ \underline{\boldsymbol{z}}^{\top} \boldsymbol{q}_{\omega 0} \geq \boldsymbol{y}_{\omega 0}^{\top} \hat{\boldsymbol{z}}_{\omega} - v_{\omega} & \forall \omega \in \Omega, \\ \boldsymbol{q}_{\omega k} = \boldsymbol{y}_{\omega k} - \boldsymbol{\nu}_{kl}(\boldsymbol{x}) & \forall \omega \in \Omega, \ k \in \mathcal{N}_l(\boldsymbol{x}), \\ \boldsymbol{q}_{\omega 0} = \boldsymbol{y}_{\omega 0} & \forall \omega \in \Omega, \\ \boldsymbol{q}_{\omega k} \geq \boldsymbol{0} & \forall \omega \in \Omega, \ k \in \mathcal{N}_l(\boldsymbol{x}) \cup \{0\}, \\ \|\boldsymbol{y}_{\omega k}\|_{\frac{p}{p-1}} \leq r & \forall \omega \in \Omega, \ k \in \mathcal{N}_l(\boldsymbol{x}) \cup \{0\} \end{cases}$$

$$\Longleftrightarrow \begin{cases} v_{\omega} \geq (\hat{\boldsymbol{z}}_{\omega} - \underline{\boldsymbol{z}})^{\top} \boldsymbol{q}_{\omega k} + \underline{\tau}_k + \boldsymbol{\nu}_{kl}(\boldsymbol{x})^{\top} \hat{\boldsymbol{z}}_{\omega} - \overline{\tau}_l + \alpha & \forall \omega \in \Omega, \ k \in \mathcal{N}_l(\boldsymbol{x}), \\ v_{\omega} \geq (\hat{\boldsymbol{z}}_{\omega} - \underline{\boldsymbol{z}})^{\top} \boldsymbol{q}_{\omega 0} & \forall \omega \in \Omega, \\ r \geq \|\boldsymbol{q}_{\omega k} + \boldsymbol{\nu}_{kl}(\boldsymbol{x})\|_{\frac{p}{p-1}} & \forall \omega \in \Omega, \ k \in \mathcal{N}_l(\boldsymbol{x}), \\ r \geq \|\boldsymbol{q}_{\omega 0}\|_{\frac{p}{p-1}} & \forall \omega \in \Omega, \\ \boldsymbol{q}_{\omega k} \geq \boldsymbol{0} & \forall \omega \in \Omega, \ k \in \mathcal{N}_l(\boldsymbol{x}) \cup \{0\}. \end{cases} \tag{EC.6}$$

The first equivalence holds by the definition of dual norm and because $\|\cdot\|_{\frac{p}{p-1}}$ is the dual norm of $\|\cdot\|_p$ (Boyd and Vandenberghe 2004); the fourth equivalence follows from linear duality.

Hence problem (EC.5) becomes

$$\begin{aligned} D_1 = \inf \ & \theta r + \frac{1}{N} \sum_{\omega \in \Omega} v_{\omega} \\ \text{s.t. } & \text{(EC.6)}, \ r \in \mathbb{R}_+, \ \boldsymbol{v} \in \mathbb{R}^{|\Omega|}, \end{aligned} \tag{EC.7}$$

a problem with only a finite number of decision variables and constraints.

Step 2: Find the closed-form solution for the term $\sup_{\mathbb{P} \in \mathcal{F}(\theta)} \mathbb{E}_{\mathbb{P}}[(\xi(\boldsymbol{x}, \tilde{\boldsymbol{z}}) + \alpha)^+]$. We proceed by making this key observation: the right-hand sides of the first four constraints in (EC.6) are increasing in $\boldsymbol{q}_{\omega k} \geq \boldsymbol{0}$ for $\omega \in \Omega$ and $k \in \mathcal{N}_l(\boldsymbol{x}) \cup \{0\}$. So as to minimize the objective function—in problem (EC.7), a weighted sum of r and $\boldsymbol{v}$—we set $\boldsymbol{q}_{\omega k} = \boldsymbol{0}$ for all $\omega \in \Omega$ and all $k \in \mathcal{N}_l(\boldsymbol{x}) \cup \{0\}$ but without changing the optimal objective value. Thus constraint (EC.6) is reduced to

$$\begin{cases} v_{\omega} \geq \underline{\tau}_k + \boldsymbol{\nu}_{kl}(\boldsymbol{x})^{\top} \hat{\boldsymbol{z}}_{\omega} - \overline{\tau}_l + \alpha & \forall \omega \in \Omega, \ k \in \mathcal{N}_l(\boldsymbol{x}), \\ v_{\omega} \geq 0 & \forall \omega \in \Omega, \\ r \geq \|\boldsymbol{\nu}_{kl}(\boldsymbol{x})\|_{\frac{p}{p-1}} & \forall \omega \in \Omega, \ k \in \mathcal{N}_l(\boldsymbol{x}), \\ r \geq 0 & \forall \omega \in \Omega. \end{cases} \tag{EC.8}$$

By definition of polynomial norm, we have $\|\boldsymbol{\nu}_{kl}(\boldsymbol{x})\|_{\frac{p}{p-1}} = |\mathcal{A}_{kl}(\boldsymbol{x})|^{\frac{p-1}{p}}$. We subsequently observe that the third constraint in (EC.8) is tightest when $k = 1$; hence this constraint is reduced to $r \geq |\mathcal{A}_{1l}(\boldsymbol{x})|^{\frac{p-1}{p}}$ (or, equivalently, to $r \geq |\mathcal{A}_l(\boldsymbol{x})|^{\frac{p-1}{p}}$) for all $\omega \in \Omega$. Note also that $\xi_l(\boldsymbol{x}, \hat{\boldsymbol{z}}_\omega) = \max_{k \in \mathcal{N}_l(\boldsymbol{x})} \{\underline{\tau}_k + \boldsymbol{\nu}_{kl}(\boldsymbol{x})' \hat{\boldsymbol{z}}_\omega - \overline{\tau}_l\}$ for $\omega \in \Omega$. It follows that problem (EC.7) has the optimal objective value

$$D_1 = \theta |\mathcal{A}_l(\boldsymbol{x})|^{\frac{p-1}{p}} + \frac{1}{N} \sum_{\omega \in \Omega} (\xi(\boldsymbol{x}, \hat{\boldsymbol{z}}_\omega) + \alpha)^+. \tag{EC.9}$$

Step 3: Substitute the closed-form result into problem (10). Recall that $D_1 = Z_1 = \sup_{\mathbb{P} \in \mathcal{F}(\theta)} \mathbb{E}_{\mathbb{P}}[(\xi_l(\boldsymbol{x}, \tilde{\boldsymbol{z}}) + \alpha_l)^+]$. We substitute (EC.9) into the first constraint of problem (10) and obtain

$$\rho_\gamma(\xi(\boldsymbol{x}, \tilde{\boldsymbol{z}})) = \min \ \alpha$$
$$\text{s.t. } \theta |\mathcal{A}_l(\boldsymbol{x})|^{\frac{p-1}{p}} + \frac{1}{N} \sum_{\omega \in \Omega} (\xi(\boldsymbol{x}, \hat{\boldsymbol{z}}_\omega) + \alpha)^+ \leq (1-\gamma)\alpha,$$
$$\alpha \geq 0.$$

Re-defining $\pi := \alpha - \frac{\theta}{1-\gamma} |\mathcal{A}_l(\boldsymbol{x})|^{\frac{p-1}{p}}$ now yields

$$\rho_\gamma(\xi(\boldsymbol{x}, \tilde{\boldsymbol{z}})) = \frac{\theta}{1-\gamma} |\mathcal{A}_l(\boldsymbol{x})|^{\frac{p-1}{p}} + \min \ \pi$$
$$\text{s.t. } \frac{1}{N} \sum_{\omega \in \Omega} \left(\xi(\boldsymbol{x}, \hat{\boldsymbol{z}}_\omega) + \frac{\theta}{1-\gamma} |\mathcal{A}_l(\boldsymbol{x})|^{\frac{p-1}{p}} + \pi \right)^+ \leq (1-\gamma)\pi,$$
$$\pi \geq -\frac{\theta}{1-\gamma} |\mathcal{A}_l(\boldsymbol{x})|^{\frac{p-1}{p}}.$$

We remark that any $\pi < 0$ would violate the first constraint and so would be infeasible. Hence we can replace the last constraint with $\pi \geq 0$ without changing the solution space. This completes the proof.

EC.1.5. Proof of Theorem 3

Theorem 2 suggests that we should focus on solving problem (11). Observe that $\bar{\rho}_{\gamma_l}(\xi_l(\boldsymbol{x}, \tilde{\boldsymbol{z}}))$ is exactly equal to the SRI for the uncertain delay *plus* a term $\frac{\theta}{1-\gamma_l} |\mathcal{A}_l(\boldsymbol{x})|^{(p-1)/p}$ under the empirical distribution $\mathbb{P}^\dagger$—that is, $\rho_{\gamma_l}\left(\xi_l(\boldsymbol{x}, \tilde{\boldsymbol{z}}^\dagger) + \frac{\theta}{1-\gamma_l} |\mathcal{A}_l(\boldsymbol{x})|^{(p-1)/p} \right)$. Using Proposition 3's property of infeasible fulfillment, we conclude that $\bar{\rho}_{\gamma_l}(\xi_l(\boldsymbol{x}, \tilde{\boldsymbol{z}})) = +\infty$ if $\text{CVAR}_{\gamma_l}\left(\xi_l(\boldsymbol{x}, \tilde{\boldsymbol{z}}^\dagger) + \frac{\theta}{1-\gamma_l} |\mathcal{A}_l(\boldsymbol{x})|^{(p-1)/p} \right) > 0$; therefore, also $\rho_{\gamma_l}(\xi_l(\boldsymbol{x}, \tilde{\boldsymbol{z}})) = +\infty$.

Otherwise, we explore the closed-form solution for problem (11). Suppressing the subscript l and putting $\hat{\xi}_\omega = \xi(\boldsymbol{x}, \hat{\boldsymbol{z}}_\omega) + \frac{\theta}{1-\gamma} |\mathcal{A}_l(\boldsymbol{x})|^{(p-1)/p}$, we can rewrite the problem as

$$\bar{\rho}_\gamma(\xi(\boldsymbol{x}, \tilde{\boldsymbol{z}})) = \min \ \alpha$$
$$\text{s.t. } \frac{1}{N} \sum_{\omega \in \Omega} \nu_\omega \leq (1-\gamma)\alpha,$$
$$\nu_\omega \geq \hat{\xi}_\omega + \alpha \qquad \forall \omega \in \Omega, \tag{EC.10}$$
$$\nu_\omega \geq 0 \qquad \forall \omega \in \Omega,$$
$$\alpha \geq 0.$$

Its dual problem is given by

$$
\begin{aligned}
D_2 = \max \quad & \sum_{\omega \in \Omega} \hat{\xi}_\omega p_\omega \\
\text{s.t.} \quad & q - \sum_{\omega \in \Omega} p_\omega \leq 1, \\
& -\frac{1}{(1-\gamma)N} q + p_\omega \leq 0 \ \forall \omega \in \Omega, \\
& q \geq 0, \\
& p_\omega \geq 0 \qquad\qquad \forall \omega \in \Omega;
\end{aligned}
\tag{EC.11}
$$

here q and $(p_\omega)_{\omega \in \Omega}$ are dual variables corresponding (respectively) to the first two constraints of problem (EC.10). Because strong duality holds for linear optimization problems, we have $\bar{\rho}_\gamma(\xi(\boldsymbol{x}, \tilde{\boldsymbol{z}})) = D_2$.

Next we prove that if $\mathrm{CVAR}_\gamma(\xi^\dagger) \leq 0$, where $\xi^\dagger$ is shorthand for $\xi(\boldsymbol{x}, \tilde{\boldsymbol{z}}^\dagger) + \frac{\theta}{1-\gamma} |\mathcal{A}_l(\boldsymbol{x})|^{(p-1)/p}$, then the optimal value of problem (EC.11) is

$$
D_2 = \max \left\{ \max_{i \in \{1,2,\dots,\lfloor (1-\gamma)N \rfloor\}} \left\{ \frac{\sum_{\omega=1}^i \hat{\xi}_{(\omega)}}{(1-\gamma)N - i} \right\}, 0 \right\},
\tag{EC.12}
$$

in which we follow the convention that $1/0 = +\infty$.

When $\hat{\xi}_{(1)} \leq 0$, we have $\hat{\xi}_\omega \leq 0$ for all $\omega \in \Omega$ and so (EC.12) becomes $D_2 = 0$. Observe that the optimal solution to problem (EC.11) is $q = 0$ and $p_\omega = 0$ for $\omega \in \Omega$ and that the objective value is $D_2 = 0$. Otherwise—that is, if $\hat{\xi}_{(1)} > 0$—we examine the optimal value based on different values of $(1-\gamma)N$ as follows.

1. If $(1-\gamma)N \leq 1$, it already falls in the above case of $\hat{\xi}_{(1)} \leq 0$; the reason is that, if $\hat{\xi}_{(1)} > 0$, then an application of formula (12) yields $\mathrm{CVAR}_\gamma(\xi^\dagger) > 0$—which contradicts our premise that $\mathrm{CVAR}_\gamma(\xi^\dagger) \leq 0$.

2. If $1 < (1-\gamma)N < N$ and $(1-\gamma)N$ is not an integer, then we obtain the optimal value by (a) constructing the primal and dual feasible solutions and (b) showing that their objective values coincide.

   Without loss of generality, we can rewrite the objective function of problem (EC.11) as $\sum_{\omega \in \Omega} \hat{\xi}_{(\omega)} p_{(\omega)}$. For any $i = 1, 2, \dots, \lfloor (1-\gamma)N \rfloor$, we construct a solution as follows. Let $p_{(\omega)} := \frac{1}{(1-\gamma)N - i}$ for $\omega = 1, 2, \dots, i$ (and $p_{(\omega)} := 0$ otherwise), and let $q := 1 + \frac{i}{(1-\gamma)N - i}$. We can verify the feasibility of the solution to problem (EC.11). The corresponding objective value is

$$
\psi(i) = \frac{\sum_{\omega=1}^i \hat{\xi}_{(\omega)}}{(1-\gamma)N - i}.
$$

Denoting $i^* := \mathrm{argmax}_{i \in \{1,2,\dots,\lfloor (1-\gamma)N \rfloor\}} \psi(i)$, we have $D_2 \geq \psi(i^*) \geq \psi(1) > 0$.

Before proceeding to construct a primal feasible solution, we first prove that $\psi(i^*) + \hat{\xi}_{(i)} \geq 0$ for $i = 1, 2, \dots, i^*$ and that $\psi(i^*) + \hat{\xi}_{(i)} \leq 0$ for $i = i^* + 1, i^* + 2, \dots, N$.

(i) If $i^* = 1$, then obviously $\psi(1) + \hat{\xi}_{(1)} > 0$. For $i^* = 2, 3, \ldots, \lfloor(1-\gamma)N\rfloor$, we have

$$
\begin{aligned}
\psi(i^*) &\geq \psi(i^* - 1) \\
&\implies \frac{\sum_{\omega=1}^{i^*} \hat{\xi}_{(\omega)}}{(1-\gamma)N - i^*} \geq \frac{\sum_{\omega=1}^{i^*} \hat{\xi}_{(\omega)} - \hat{\xi}_{(i^*)}}{(1-\gamma)N - i^* + 1}, \\
&\implies \frac{\sum_{\omega=1}^{i^*} \hat{\xi}_{(\omega)}}{(1-\gamma)N - i^*} \geq -\hat{\xi}_{(i^*)}, \\
&\implies \psi(i^*) + \hat{\xi}_{(i^*)} \geq 0, \\
&\implies \psi(i^*) + \hat{\xi}_{(i)} \geq 0 \quad \forall i = 1, 2, \ldots, i^*.
\end{aligned}
\tag{EC.13}
$$

The last implication follows from the monotonicity of $\hat{\xi}_{(i)}$.

(ii) For $i^* = 1, 2, \ldots, \lfloor(1-\gamma)N\rfloor - 1$, we similarly obtain

$$
\begin{aligned}
\psi(i^*) &\geq \psi(i^* + 1) \\
&\implies \frac{\sum_{\omega=1}^{i^*} \hat{\xi}_{(\omega)}}{(1-\gamma)N - i^*} \geq \frac{\sum_{\omega=1}^{i^*} \hat{\xi}_{(\omega)} + \hat{\xi}_{(i^*+1)}}{(1-\gamma)N - i^* - 1}, \\
&\implies -\frac{\sum_{\omega=1}^{i^*} \hat{\xi}_{(\omega)}}{(1-\gamma)N - i^*} \geq \hat{\xi}_{(i^*+1)}, \\
&\implies \psi(i^*) + \hat{\xi}_{(i^*+1)} \leq 0, \\
&\implies \psi(i^*) + \hat{\xi}_{(i)} \leq 0 \quad \forall i = i^* + 1, i^* + 2, \ldots, N.
\end{aligned}
\tag{EC.14}
$$

If $i^* = \lfloor(1-\gamma)N\rfloor$, then

$$
\begin{aligned}
\text{CVAR}_\gamma(\xi^\dagger) &\leq 0 \\
&\implies \sum_{\omega=1}^{i^*} \hat{\xi}_{(\omega)} + ((1-\gamma)N - i^*)\hat{\xi}_{(i^*+1)} \leq 0, \\
&\implies \psi(i^*) + \hat{\xi}_{(i^*+1)} \leq 0, \\
&\implies \psi(i^*) + \hat{\xi}_{(i)} \leq 0 \quad \forall i = i^* + 1, i^* + 2, \ldots, N.
\end{aligned}
\tag{EC.15}
$$

We now argue that $\alpha := \psi(i^*)$ is a feasible solution to problem (EC.10). We have

$$
\begin{aligned}
&\frac{\sum_{\omega=1}^{i^*} \hat{\xi}_{(\omega)}}{(1-\gamma)N - i^*} \leq \frac{\sum_{\omega=1}^{i^*} \hat{\xi}_{(\omega)}}{(1-\gamma)N - i^*} \\
&\implies \frac{1}{(1-\gamma)N}\left(\frac{((1-\gamma)N - i^*)\sum_{\omega=1}^{i^*} \hat{\xi}_{(\omega)}}{(1-\gamma)N - i^*} + \frac{i^* \sum_{\omega=1}^{i^*} \hat{\xi}_{(\omega)}}{(1-\gamma)N - i^*}\right) \leq \frac{\sum_{\omega=1}^{i^*} \hat{\xi}_{(\omega)}}{(1-\gamma)N - i^*} \\
&\implies \frac{1}{(1-\gamma)N}\left(\sum_{\omega=1}^{i^*} \hat{\xi}_{(\omega)} + i^*\psi(i^*)\right) \leq \psi(i^*) \\
&\implies \frac{1}{N}\sum_{\omega\in\Omega}(\hat{\xi}_{(\omega)} + \psi(i^*))^+ \leq (1-\gamma)\psi(i^*) \\
&\implies \frac{1}{N}\sum_{\omega\in\Omega}(\hat{\xi}_{(\omega)} + \alpha)^+ \leq (1-\gamma)\alpha.
\end{aligned}
$$

The third implication holds owing to (EC.13)–(EC.15). It follows that such an α is a feasible solution to problem (EC.10) and that $\bar{\rho}_\gamma(\xi(\boldsymbol{x}, \tilde{\boldsymbol{z}})) \leq \psi(i^*)$.

In summary, we have $\psi(i^*) \leq D_2 \leq \bar{\rho}_\gamma(\xi(\boldsymbol{x}, \tilde{\boldsymbol{z}})) \leq \psi(i^*)$. Therefore, the feasible solutions to the primal and dual problems are indeed optimal and have the same objective value,

$$D_2 = \psi(i^*) = \max_{i \in \{1,2,\ldots,\lfloor(1-\gamma)N\rfloor\}} \left\{ \frac{\sum_{\omega=1}^{i} \hat{\xi}_{(\omega)}}{(1-\gamma)N - i} \right\}.$$

(iii) Suppose that $(1-\gamma)N = 2, 3, \ldots, N$. Then, since $(1-\gamma)N - \lfloor(1-\gamma)N\rfloor = 0$ cannot be the denominator, we must tailor the proof as follows to obtain the desired result.

For any $i = 1, 2, \ldots, \lfloor(1-\gamma)N\rfloor - 1$, a solution is constructed as before; that is, $p_{(\omega)} := \frac{1}{(1-\gamma)N-i}$ for $\omega = 1, 2, \ldots, i$ (and $p_{(\omega)} := 0$ otherwise) and $q := 1 + \frac{i}{(1-\gamma)N-i}$. Hence this solution is applicable also to problem (EC.11). If we put $i^* := \mathrm{argmax}_{i \in \{1,2,\ldots,\lfloor(1-\gamma)N\rfloor-1\}} \psi(i)$, then $D_2 \geq \psi(i^*) > 0$.

Before proceeding to construct a primal feasible solution, we again first prove that $\psi(i^*) + \hat{\xi}_{(i)} \geq 0$ for $i = 1, 2, \ldots, i^*$ and that $\psi(i^*) + \hat{\xi}_{(i)} \leq 0$ for $i = i^*+1, i^*+2, \ldots, N$. If $i^* = 1$ then clearly $\psi(1) + \hat{\xi}_{(1)} > 0$. For $i^* = 2, 3, \ldots, \lfloor(1-\gamma)N\rfloor - 1$, we follow the preceding proof to obtain that $\psi(i^*) \geq \psi(i^* - 1)$ implies $\psi(i^*) + \hat{\xi}_{(i)} \geq 0$ for all $i = 1, 2, \ldots, i^*$. Similarly, for $i^* = 1, 2, \ldots, \lfloor(1-\gamma)N\rfloor - 2$ we have that $\psi(i^*) \geq \psi(i^* + 1)$ implies $\psi(i^*) + \hat{\xi}_{(i)} \leq 0$ for all $i = i^*+1, i^*+2, \ldots, N$. When $i^* = \lfloor(1-\gamma)N\rfloor - 1$, the following new proof is needed. We have

$$\mathrm{CVAR}_\gamma(\xi^\dagger) \leq 0$$
$$\implies \sum_{\omega=1}^{\lfloor(1-\gamma)N\rfloor} \hat{\xi}_{(\omega)} \leq 0,$$
$$\implies \frac{\sum_{\omega=1}^{i^*} \hat{\xi}_{(\omega)}}{(1-\gamma)N - i^*} + \hat{\xi}_{(\lfloor(1-\gamma)N\rfloor)} \leq 0,$$
$$\implies \psi(i^*) + \hat{\xi}_{(i)} \leq 0 \quad \forall i = i^*+1, i^*+2, \ldots, N.$$

The second implication holds because $(1-\gamma)N - i^* = (1-\gamma)N - \lfloor(1-\gamma)N\rfloor + 1 = 1$. Finally, we follow the above proof and know that $\alpha := \psi(i^*)$ is a feasible solution to problem (EC.10). Therefore,

$$D_2 = \psi(i^*) = \max_{i \in \{1,2,\ldots,\lfloor(1-\gamma)N\rfloor-1\}} \left\{ \frac{\sum_{\omega=1}^{i} \hat{\xi}_{(\omega)}}{(1-\gamma)N - i} \right\} = \max_{i \in \{1,2,\ldots,\lfloor(1-\gamma)N\rfloor\}} \left\{ \frac{\sum_{\omega=1}^{i} \hat{\xi}_{(\omega)}}{(1-\gamma)N - i} \right\}.$$

The last implication holds because

$$\frac{\sum_{\omega=1}^{\lfloor(1-\gamma)N\rfloor} \hat{\xi}_{(\omega)}}{(1-\gamma)N - \lfloor(1-\gamma)N\rfloor} = \sum_{\omega=1}^{\lfloor(1-\gamma)N\rfloor} \hat{\xi}_{(\omega)} \times \infty = -\infty.$$

Taking all these situations into account, we have proved the closed-form solution (EC.12).

Hence we can use the result and obtain

$$\rho_{\gamma_l}(\xi_l(\boldsymbol{x}, \tilde{\boldsymbol{z}})) = \frac{\theta}{1-\gamma_l}|\mathcal{A}_l(\boldsymbol{x})|^{(p-1)/p} + D_2$$

$$= \frac{\theta}{1-\gamma_l}|\mathcal{A}_l(\boldsymbol{x})|^{(p-1)/p}$$

$$+ \max\left\{\max_{i\in\{1,2,\ldots,\lfloor(1-\gamma_l)N\rfloor\}}\left\{\frac{\sum_{\omega=1}^{i}\left(\xi_l(\boldsymbol{x}, \hat{\boldsymbol{z}}_{(\omega)}) + \frac{\theta}{1-\gamma_l}|\mathcal{A}_l(\boldsymbol{x})|^{(p-1)/p}\right)}{(1-\gamma_l)N - i}\right\}, 0\right\}.$$

The result then follows.

EC.1.6. Proof of Theorem 4

If we apply the result of Theorem 2 to problem (15), then the VRPTW becomes

$$Z = \sum_{l\in\mathcal{N}}\frac{\theta|\mathcal{A}_l(\boldsymbol{x})|^{\frac{p-1}{p}}}{1-\gamma_l} + \min\sum_{l\in\overline{\mathcal{N}}}\alpha_l,$$

$$\text{s.t.} \quad \frac{1}{N}\sum_{\omega\in\Omega}\left(\xi_l(\boldsymbol{x}, \hat{\boldsymbol{z}}_\omega) + \frac{\theta|\mathcal{A}_l(\boldsymbol{x})|^{\frac{p-1}{p}}}{1-\gamma_l} + \alpha_l\right)^+ \leq (1-\gamma_l)\alpha_l \ \forall l\in\overline{\mathcal{N}}, \quad \text{(EC.16)}$$

$$\alpha_l \geq 0 \qquad\qquad\qquad\qquad\qquad\qquad\qquad\qquad\qquad \forall l\in\overline{\mathcal{N}},$$

$$\boldsymbol{c}^\top\boldsymbol{x} \leq B,$$

$$\boldsymbol{x} \in \mathcal{X}.$$

Consider the ℓ_1 norm in our definition (9) of the Wasserstein distance. We have $p = 1$ and so $|\mathcal{A}_l(\boldsymbol{x})|^{(p-1)/p} = 1$ for all $l\in\overline{\mathcal{N}}$. Problem (EC.16) then reduces to

$$Z = \sum_{l\in\overline{\mathcal{N}}}\frac{\theta}{1-\gamma_l} + \min\sum_{l\in\overline{\mathcal{N}}}\alpha_l,$$

$$\text{s.t.} \quad \frac{1}{N}\sum_{\omega\in\Omega}\left(\left(\xi_l(\boldsymbol{x}, \hat{\boldsymbol{z}}_\omega) + \frac{\theta}{1-\gamma_l}\right) + \alpha_l\right)^+ \leq (1-\gamma_l)\alpha_l \ \forall l\in\overline{\mathcal{N}}, \quad \text{(EC.17)}$$

$$\alpha_l \geq 0 \qquad\qquad\qquad\qquad\qquad\qquad\qquad\qquad \forall l\in\overline{\mathcal{N}},$$

$$\boldsymbol{c}^\top\boldsymbol{x} \leq B,$$

$$\boldsymbol{x} \in \mathcal{X}.$$

The condition $\overline{\tau}_1 = +\infty$ indicates that $\overline{\mathcal{N}}$ comprises all customer locations with deadlines, which is a fixed set. Hence $\sum_{l\in\overline{\mathcal{N}}}\frac{\theta}{1-\gamma_l}$ is a constant value.

Comparing (EC.17) with the VRPTW (16) under the empirical distribution, we conclude that the former differs from the latter only in (a) adding a constant value (in the objective function) that does not affect the optimal solution and (b) adding (in the first constraint) a constant value $\frac{\theta}{1-\gamma_l}$ to $\xi_l(\boldsymbol{x}, \hat{\boldsymbol{z}}_\omega)$ for all $l\in\overline{\mathcal{N}}$ and $\omega\in\Omega$. Given that $\xi_l(\boldsymbol{x}, \hat{\boldsymbol{z}}_\omega) + \frac{\theta}{1-\gamma_l} = t_l(\boldsymbol{x}, \hat{\boldsymbol{z}}_\omega) - \left(\overline{\tau}_l - \frac{\theta}{1-\gamma_l}\right)$, we obtain the result.

EC.1.7. Proof of Proposition 4

Toth and Vigo (2014) demonstrate that, in constraint (18), the decision variable v_i represents the "service start time" at node $i \in \mathcal{N}$ in the deterministic world. It remains to prove that our SRI would imply $v_i \le \overline{\tau}_i$ ($i \in \mathcal{N}$) so that adding constraint (18) does not remove any feasible $\boldsymbol{x}$.

As given in Proposition 3, the infeasible fulfillment property of SRI implies that a feasible solution $\boldsymbol{x}$ should satisfy the inequality $\mathcal{F}\text{-CVAR}_\gamma(\xi_i(\boldsymbol{x}, \tilde{\boldsymbol{z}})) \le 0$. For $i \in \mathcal{N}$, we also have that

$$\mathcal{F}\text{-CVAR}_\gamma(\xi_i(\boldsymbol{x}, \tilde{\boldsymbol{z}})) \le 0$$
$$\implies \mathcal{F}\text{-CVAR}_\gamma(t_i(\boldsymbol{x}, \tilde{\boldsymbol{z}}) - \overline{\tau}_i) \le 0$$
$$\implies \mathcal{F}\text{-CVAR}_\gamma(t_i(\boldsymbol{x}, \tilde{\boldsymbol{z}})) \le \overline{\tau}_i$$
$$\implies \mathcal{F}\text{-CVAR}_0(t_i(\boldsymbol{x}, \tilde{\boldsymbol{z}})) \le \overline{\tau}_i$$
$$\implies \mathbb{E}_\mathbb{P}[t_i(\boldsymbol{x}, \tilde{\boldsymbol{z}})] \le \overline{\tau}_i$$
$$\implies v_i \le \overline{\tau}_i.$$

These five implications result, respectively, from: our definition (3) of the delay function, the translation invariance of CVAR, the fact that CVAR does not decrease with γ; the equality $\mathcal{F}\text{-CVAR}_0(t_i(\boldsymbol{x}, \tilde{\boldsymbol{z}})) = \mathbb{E}_\mathbb{P}[t_i(\boldsymbol{x}, \tilde{\boldsymbol{z}})]$; and Proposition 2. The properties of CVAR cited here are established in Rockafellar and Uryasev (2002).

EC.1.8. Proof of Proposition 5

Consider a route $(1, i_2, i_3, \ldots, i, j, l, \ldots, i_\nu)$, where $l \in \overline{\mathcal{N}}$ and $i_\nu \in \mathcal{N}_d$. We know from Theorem 3 that the route is infeasible if, for any l,

$$\text{CVAR}_{\gamma_l}\left(\xi_l(\boldsymbol{x}, \tilde{\boldsymbol{z}}^\dagger) + \frac{\theta}{1 - \gamma_l}|\mathcal{A}_l(\boldsymbol{x})|^{\frac{p-1}{p}}\right) > 0.$$

By definition of the delay function (3), if we put $k := j$ and $k := i$, respectively, then

$$\xi_l(\boldsymbol{x}, \tilde{\boldsymbol{z}}^\dagger) \ge \max\{\underline{\tau}_j + \tilde{z}_{jl}^\dagger, \underline{\tau}_l\} - \overline{\tau}_l$$

and

$$\xi_l(\boldsymbol{x}, \tilde{\boldsymbol{z}}^\dagger) \ge \max\left\{\underline{\tau}_i + \tilde{z}_{ij}^\dagger + \tilde{z}_{jl}^\dagger, \underline{\tau}_j + \tilde{z}_{jl}^\dagger, \underline{\tau}_l\right\} - \overline{\tau}_l.$$

Considering the facts that (i) $|\mathcal{A}_l(\boldsymbol{x})|^{(p-1)/p} \ge 1$ because $|\mathcal{A}_l(\boldsymbol{x})| \ge 1$ and $\frac{p-1}{p} \ge 0$, and (ii) $\text{CVAR}_{\gamma_l}(\tilde{v})$ is nondecreasing in $\tilde{v}$, we conclude that if

$$\text{CVAR}_{\gamma_l}\left(\max\{\underline{\tau}_j + \tilde{z}_{jl}^\dagger, \underline{\tau}_l\} - \overline{\tau}_l + \frac{\theta}{1 - \gamma_l}\right) > 0$$

then (i) $\text{CVAR}_{\gamma_l}\left(\xi_l(\boldsymbol{x}, \tilde{\boldsymbol{z}}^\dagger) + \frac{\theta}{1 - \gamma_l}|\mathcal{A}_l(\boldsymbol{x})|^{(p-1)/p}\right) > 0$ and (ii) any route passing through arc (j, l) is infeasible. We therefore let $x_{jl} = 0$. By the same token, if

$$\text{CVAR}_{\gamma_l}\left(\max\left\{\max\{\underline{\tau}_i + \tilde{z}_{ij}^\dagger, \underline{\tau}_j\} + \tilde{z}_{jl}^\dagger, \underline{\tau}_l\right\} - \overline{\tau}_l + \frac{\theta}{1 - \gamma_l}\right) > 0,$$

then any route that passes the consecutive arcs (i, j) and (j, l) is infeasible and so $x_{ij} + x_{jl} \le 1$.

EC.2. Example of Expected Service Start Time

To illustrate Proposition 2, we provide an example in Figure EC.1. Consider the route from node 1 to node 2 to node 3. In deterministic models, the travel times are the mean values; hence, at time 2, a vehicle can arrive and start the service on time at node 3. In the uncertain world, however, the arrival time at node 3 is $\max\{0.5,1\}+1.2=2.2$ with probability $1/2$ and is 2.3 with probability $1/2$. It follows that the mean value of the uncertain service start time is 2.25—which is underestimated by an arrival time of 2. It is crucial to our argument that the vehicle's probability of on-time arrival is 0. We must conclude that ignoring uncertainty in vehicle routing can lead to poor service with regard to time windows.
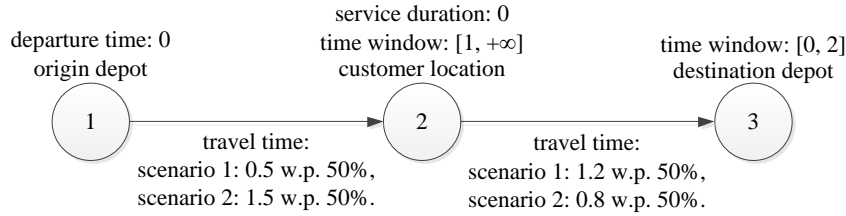

Figure EC.1   Example misconception of expected service start time (w.p. = "with probability")

EC.3. Multi-commodity Flow Formulation

Here we propose an alternative multi-commodity flow formulation for our VRPTW. In addition to the $\boldsymbol{x}$ introduced in Section 2 to represent a feasible routing solution, we also use the continuous decision variables $\boldsymbol{s} = (s_a^l)_{l\in\mathcal{N}, a\in\mathcal{A}}$ to trace the routes from depot 1 to nodes in $\mathcal{N}$. Thus we define the feasible region of $(\boldsymbol{x}, \boldsymbol{s})$ by

$$
\mathcal{S} = \left\{
\begin{array}{l}
\boldsymbol{x}\in\{0,1\}^{|\mathcal{A}|}, \\[2mm]
\boldsymbol{s}\in\mathbb{R}_+^{|\mathcal{N}|\times|\mathcal{A}|}
\end{array}
\left|
\begin{array}{ll}
\displaystyle\sum_{a\in\delta^+(i)} x_a = \sum_{a\in\delta^-(i)} x_a = 1, & i\in\mathcal{N}_c; \\[4mm]
\displaystyle\sum_{a\in\delta^+(1)} x_a \le m; & \\[4mm]
\displaystyle\sum_{a\in\delta^-(i)} x_a \le 1, & i\in\mathcal{N}_d; \\[4mm]
s_a^1 = 0, & a\in\mathcal{A}; \\[1mm]
s_a^l \le x_a, & l\in\mathcal{N}_c\cup\mathcal{N}_d, a\in\mathcal{A}; \\[1mm]
\displaystyle\sum_{a\in\delta^+(1)} s_a^l = \sum_{a\in\delta^-(l)} s_a^l = \sum_{a\in\delta^-(l)} x_a, & l\in\mathcal{N}_c\cup\mathcal{N}_d; \\[4mm]
\displaystyle\sum_{a\in\delta^+(l)} s_a^l = 0, & l\in\mathcal{N}_c; \\[4mm]
\displaystyle\sum_{a\in\delta^+(i)} s_a^l - \sum_{a\in\delta^-(i)} s_a^l = 0, & l\in\mathcal{N}_c, i\in\mathcal{N}_c\backslash\{l\}; \\[4mm]
\displaystyle\sum_{(i,j)\in\mathcal{A}} q_i s_{ij}^l \le Q, & l\in\mathcal{N}_d
\end{array}
\right.
\right\}.
\tag{EC.18}
$$

The first three constraints in (EC.18) are the same as those in (1); explanations for these constraints are given in Section 2. The next five constraints, in the spirit of Adulyasak and Jaillet (2015), eliminate subtours and trace the partial route from depot 1 to any node $l \in \mathcal{N}$. Last is the capacity constraint. Note that, given the variables $\boldsymbol{s}$ and their constraints, we need not posit rounded capacity inequalities such as those appearing in (1).

In set $\mathcal{S}$, the decision variables $\boldsymbol{x}$ determine a feasible routing solution and $\boldsymbol{s}^l$ $(l \in \mathcal{N}_c \cup \mathcal{N}_d)$ corresponds to the partial route—along one of the routes determined by $\boldsymbol{x}$—from depot 1 to node l. We specify this route using $(1, i_2, i_3, \ldots, i_{\kappa-1}, i_\kappa, \ldots, i_{\nu-1}, i_\nu)$, which passes through node $l = i_\kappa$ and ends at node $i_\nu \in \mathcal{N}_d$. Then

$$s_a^l = \begin{cases} 1 & \text{if } a \in \{(1, i_2), (i_2, i_3), \ldots, (i_{\kappa-1}, l)\}, \\ 0 & \text{otherwise.} \end{cases} \tag{EC.19}$$

Hence the continuous decision variables $\boldsymbol{s}$ must be binary.

The representation $\mathcal{S}$ for the VRPTW is inspired by the work of Adulyasak and Jaillet (2015) and Zhang et al. (2019a). In particular, Zhang et al. (2019a) extend the TSP formulation of Claus (1984) to the TSPTW, and we extend Zhang et al. (2019a) to the VRPTW case. Although Adulyasak and Jaillet (2015) also formulate a multi-commodity flow formulation for the VRPTW, they pose exponentially many rounded capacity inequalities; in contrast, our approach requires only polynomially many constraints and therefore yields a more compact formulation.

For the studied TSPTW, Zhang et al. (2019a) represent the service start time at the given node as a convex piecewise affine function in the travel times along arcs and in the decision variables. We now establish the intriguing result that, although the VRPTW is generally more complicated than the TSPTW, the same representation is valid for both.

Proposition 6 *Suppose we are given a routing solution $(\boldsymbol{x}, \boldsymbol{s}) \in \mathcal{S}$ and a realization $\boldsymbol{z}$ of travel times $\tilde{\boldsymbol{z}}$. Then the service start time for each node $l \in \mathcal{N}$ is determined by the function*

$$t_l(\boldsymbol{x}, \boldsymbol{z}) = \max_{k \in \underline{\mathcal{N}} \cup \{1\}} \left\{ \sum_{a \in \delta^-(k)} s_a^l \underline{\tau}_k + \boldsymbol{z}^\top (\boldsymbol{x}^l - \boldsymbol{x}^k) \right\}. \tag{EC.20}$$

Proof: The proof is extended from Zhang et al. (2019a). Recall that we can use (EC.1) to represent the service start time at node $l \in \mathcal{N}$; that is,

$$t_l = \max_{k \in \{1, i_2, i_3, \ldots, i_{\kappa-1}, l\}} \left\{ \underline{\tau}_k + \sum_{a \in \{(k, i_{\upsilon+1}), (i_{\upsilon+1}, i_{\upsilon+2}), \ldots, (i_{\kappa-1}, l)\}} z_a \right\}, \tag{EC.21}$$

where $k = i_\upsilon$ is a node along the path from node 1 to node l.

Next we show the equivalence of our formulations (EC.20) and (EC.21). We put $t_l^k = \sum_{a \in \delta^-(k)} s_a^l \underline{\tau}_k + \boldsymbol{z}^\top (\boldsymbol{s}^l - \boldsymbol{s}^k)$ for $k \in \underline{\mathcal{N}} \cup \{1\}$ and discuss three separate cases as follows.

1. When $k = 1$, we have $\underline{\tau}_1 = 0$ and $\boldsymbol{s}^1 = \boldsymbol{0}$; therefore,

$$t_l^1 = \sum_{a \in \delta^-(1)} s_a^l \underline{\tau}_1 + \boldsymbol{z}^\top(\boldsymbol{s}^l - \boldsymbol{s}^1) = \boldsymbol{z}^\top \boldsymbol{s}^l = \underline{\tau}_1 + \sum_{a \in \{(1,i_2),(i_2,i_3),\ldots,(i_{\kappa-1},l)\}} z_a.$$

Note that $t_l^1 \geq 0$ because $\boldsymbol{z} \geq \boldsymbol{0}$ and $\boldsymbol{s}^l \geq \boldsymbol{0}$.

2. When $k \in \{i_2, i_3, \ldots, i_{\kappa-1}, l\} \cap \underline{\mathcal{N}}$, we have $\sum_{a \in \delta^-(k)} s_a^l = 1$ and

$$t_l^k = \sum_{a \in \delta^-(k)} s_a^l \underline{\tau}_k + \boldsymbol{z}^\top(\boldsymbol{s}^l - \boldsymbol{s}^k) = \underline{\tau}_k + \sum_{a \in \{(k,i_{\upsilon+1}),(i_{\upsilon+1},i_{\upsilon+2}),\ldots,(i_{\kappa-1},l)\}} z_a.$$

3. When $k \in \underline{\mathcal{N}} \setminus \{i_2, i_3, \ldots, i_{\kappa-1}, l\}$, we have $\sum_{a \in \delta^-(k)} s_a^l = 0$. Therefore,

$$t_l^k = \sum_{a \in \delta^-(k)} s_a^l \underline{\tau}_k + \boldsymbol{z}^\top(\boldsymbol{s}^l - \boldsymbol{s}^k) \leq \boldsymbol{z}^\top \boldsymbol{s}^l \leq t_l^1.$$

The result then follows.   □

Now the delay function can be written as

$$\xi_l(\boldsymbol{s}, \boldsymbol{z}) = t_l(\boldsymbol{s}, \boldsymbol{z}) - \overline{\tau}_l \qquad\qquad (\text{EC.22})$$

and the VRPTW formulation as

$$\begin{aligned} \min \sum_{l \in \mathcal{N}} \rho_{\gamma_l}(\xi_l(\boldsymbol{s}, \tilde{\boldsymbol{z}})) \\ \text{s.t. } \boldsymbol{c}^\top \boldsymbol{x} \leq B, \\ (\boldsymbol{x}, \boldsymbol{s}) \in \mathcal{S}. \end{aligned} \qquad\qquad (\text{EC.23})$$

In comparison with (4), the advantage of formulation (EC.23) lies mainly in its compactness. Hence solutions can be derived via general-purpose solvers and without resorting to sophisticated approaches, so non-experts may be encouraged to use this approach to solve small instances. That said, the intrinsic complexity of (EC.23) means that one must design sophisticated approaches to solve larger instances. Because this formulation involves $|\mathcal{N}| \times |\mathcal{A}|$ more decision variables $\boldsymbol{s}$, it could be computationally burdensome to solve the linear relaxations in a branch-and-bound tree. According to our simulations in Section 7, (4) can be solved more efficiently by the branch-and-cut approach described in Section 5 than by (EC.23) when solved via the Benders decomposition approach discussed below.

Observe that the structure of (EC.23) is similar to the formulation of Zhang et al. (2019a). One can work out a Benders decomposition approach to solve (EC.23) in the framework proposed by Zhang et al. (2019a). In particular, when fixing the values of decision variables $(\boldsymbol{x}, \boldsymbol{s})$ in the restricted master problem, solving the subproblem for each $l \in \overline{\mathcal{N}}$ is tantamount to evaluating the SRI $\rho_{\gamma_l}(\xi_l(\boldsymbol{s}, \tilde{\boldsymbol{z}}))$—for which the closed-form solution is readily available from Theorem 3. We omit the details and leave the spelling out of a Benders decomposition approach as an exercise for readers.

EC.4. Impact of Distributions

Apart from the two-point distribution, we also test the cases of uniform and triangular distributions of travel times (Adulyasak and Jaillet 2015, Errico et al. 2016). Toward that end, for each arc $a \in \mathcal{A}$ we keep the same mean μ_a and standard deviation σ_a as in the two-point distribution; thus the uniform distribution is supported on $[\mu_a - \sqrt{3}\sigma_a, \mu_a + \sqrt{3}\sigma_a]$. We generate an asymmetric triangular distribution by setting its lower limit at $\mu_a - (5/3)\sqrt{(18/13)}\sigma_a$, its upper limit at $\mu_a - (2/3)\sqrt{(18/13)}\sigma_a$, and its mode at $\mu_a + (7/3)\sqrt{(18/13)}\sigma_a$. Until now, we have assumed independent distributions. To test the impact of correlations in distributions, we generate correlated travel times from the two-point distribution case by adding—for each arc $a \in \mathcal{A}$—a correlated term $k_a\tilde{\varepsilon}$ to each travel time $\tilde{z}_a$. We divide the map uniformly into urban, suburban, and exurban areas based on their relative centrality; the central area's greater congestion is captured by putting $k_a = 1$ for an urban arc, $k = 0$ for a suburban arc, and $k = -1$ for an exurban arc. The random noise $\tilde{\varepsilon}$ can model any factor (e.g., the weather) that affects all travel times simultaneously. In our experiment, the noise $\tilde{\varepsilon}$ follows a uniform distribution in $[0, \sigma_a]$. The results are reported in Table EC.1.

We can see that the results are much the same across the various distribution cases. Readers are therefore referred to Section 7 for related analysis and discussion.

Table EC.1   Tests on different distributions

Distribution	Instance	Method	Performance							
			Cost	*nLate*	*MaxProb*	*SumProb*	*MaxExp*	*SumExp*	*Early*	*CPU*
Two-point	r1	I	1.049	0.00	0.296	2.558	2.41	12.64	540	522
		E	1.049	2.83	0.843	4.900	5.82	25.89	492	378
		P	1.049	3.25	0.981	4.816	60.99	151.30	550	305
	c1	I	1.038	0.00	0.092	0.310	0.42	0.95	238	21
		E	1.042	0.00	0.092	0.310	0.42	0.95	174	49
		P	1.040	0.00	0.088	0.306	0.42	1.02	327	74
	rc1	I	1.051	0.00	0.337	3.217	4.02	20.92	452	374
		E	1.048	2.88	0.757	4.847	8.19	32.42	383	529
		P	1.048	2.63	0.920	4.029	71.93	132.76	454	400
Uniform	r1	I	1.049	0.00	0.333	1.964	1.61	6.51	541	573
		E	1.049	2.92	0.892	4.723	6.39	22.00	444	383
		P	1.048	3.58	1.000	4.616	85.47	178.23	497	475
	c1	I	1.037	0.00	0.036	0.085	0.14	0.23	202	70
		E	1.043	0.00	0.036	0.085	0.14	0.23	180	48
		P	1.045	0.00	0.036	0.085	0.14	0.23	284	69
	rc1	I	1.052	0.00	0.358	3.008	2.91	15.51	436	564
		E	1.049	2.25	0.825	4.443	8.46	28.01	381	367
		P	1.048	2.38	1.000	3.734	65.70	130.97	427	513
Triangular	r1	I	1.050	0.00	0.298	2.375	1.77	9.92	513	645
		E	1.049	3.42	0.858	4.933	10.09	27.48	462	295
		P	1.049	3.42	0.965	4.748	74.49	187.27	546	433
	c1	I	1.038	0.00	0.045	0.208	0.29	0.99	223	57
		E	1.045	0.00	0.045	0.209	0.29	0.99	162	58
		P	1.044	0.00	0.045	0.208	0.29	0.99	285	84
	rc1	I	1.050	0.00	0.340	2.722	2.84	15.86	430	401
		E	1.049	2.38	0.860	4.043	9.67	29.33	429	643
		P	1.049	2.88	1.000	3.935	54.84	99.71	408	410
Correlated	r1	I	1.049	0.00	0.267	2.301	1.92	9.98	529	487
		E	1.049	2.92	0.933	4.820	6.79	24.30	475	284
		P	1.048	4.00	0.964	4.867	71.83	186.93	531	448
	c1	I	1.037	0.00	0.088	0.284	0.40	0.87	176	58
		E	1.044	0.00	0.088	0.284	0.40	0.87	193	102
		P	1.041	0.00	0.084	0.278	0.40	0.92	175	71
	rc1	I	1.051	0.00	0.324	3.159	4.03	21.56	478	488
		E	1.049	3.00	0.917	4.406	7.93	28.50	463	297
		P	1.048	3.38	0.975	4.191	55.06	120.51	444	537